

DESTRUCTION OF ETHYLENE IN A LIQUID  
ELECTRODE PLASMA REACTOR

By

THOMAS KEITH GRAHAM

Bachelor of Science

Oklahoma State University

Stillwater, Oklahoma

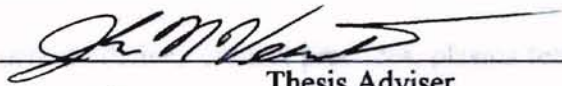
1995

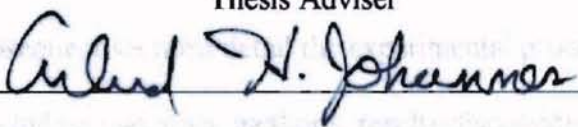
Submitted to the Faculty of the  
Graduate College of the  
Oklahoma State University  
in partial fulfillment of  
the requirements for  
the Degree of  
MASTER OF SCIENCE  
May, 1997

**DESTRUCTION OF ETHYLENE IN A LIQUID  
ELECTRODE PLASMA REACTOR**


The purpose behind this thesis was to explore the use of plasma technology in the  
and of the industry and to contribute to the pool of plasma knowledge at Oklahoma  
State University. This project was a joint venture between the School of Biosystems and  
Engineering and the School of Civil and Environmental Engineering.

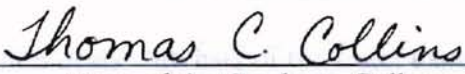
**Thesis Approved:**

  
\_\_\_\_\_  
Thesis Adviser

  
\_\_\_\_\_  
Arthur H. Johannes

  
\_\_\_\_\_  
Paul Amstrong

  
\_\_\_\_\_  
Gregory J. Wilber

  
\_\_\_\_\_  
Dean of the Graduate College

OKLAHOMA STATE UNIVERSITY

## PREFACE

The purpose behind this thesis was to explore the use of plasma technology in the food storage industry and to contribute to the pool of plasma knowledge at Oklahoma State University. The project was a joint venture between the School of Biosystems and Agricultural Engineering and the School of Civil and Environmental Engineering.

The report is organized into several sections. The first section, the introduction, defines the problem of ethylene production in produce facilities. This section also gives a background for current ethylene control practices, plasma technology, and objectives of the research. The subsequent sections detail the experimental process followed to meet research objectives including materials, methods, results/discussion, and conclusions/recommendations.

The materials section outlines various apparatus used during the research. Each experiment is detailed and defined to allow future researchers to repeat the experimental setups. The methods section deals with lists of the exact experimental procedures and should give exact details for repetition of entire experiments. Finally, the results/discussion and conclusions/recommendations sections are intended to present research findings and assess its successes, failures, short-comings, and needs for improvements. In summary, the entire document is intended as a complete base study for future researchers to use and expand upon.

## ACKNOWLEDGMENTS

I wish to express my sincere appreciation to Dr. John Veenstra and Paul Armstrong. Their willingness to give advice and much needed equipment has been essential to the success of this project. They have both provided insights and experiences that have helped me out of several dilemmas. Without the two of them to listen to and critique my sometimes off-the-wall ideas, this research would have never proceeded beyond its initial phase.

I would also like to thank others who have contributed advice and materials along the way. Without plenty of both, the entire process would have been much more difficult. The list of contributors is too long to mention, but you know who you are. My gratitude is also extended to the School of Biosystems and Agricultural Engineering for its contribution to funding my work. I also wish to express a special thanks to my friends and family who have had to put up with me throughout this entire process. Especially to those who always ask how my research was going even when they did not want to hear an hour long rendition of my latest findings.

Finally, I wish to thank the School of Civil and Environmental Engineering and the College of Engineering, Architecture, and Technology. The friendships I have developed over the past six years with its faculty and staff, both in and out of the classroom, will be cherished my entire life.



.....	53
.....	55
.....	68

## TABLE OF CONTENTS

<b>Introduction.....</b>	<b>1</b>
Ethylene Problem.....	1
Plasma Physics.....	5
Things Proved and To Be Proved.....	7
<b>Materials.....</b>	<b>9</b>
Plasma System.....	9
Electronics.....	12
Thermistors.....	13
Other Common Elements.....	15
Temperature System.....	16
Ozone System.....	17
Single Pass System.....	18
Closed Loop System.....	19
Analysis Equipment.....	21
<b>Methods.....</b>	<b>23</b>
Plasma Optimization.....	23
Temperature Experiments.....	26
Ozone Experiments.....	27
Single Pass Ethylene Destruction Experiments.....	28
Closed Loop Ethylene Destruction Experiments.....	29
By-Product Identification Experiment.....	30
Special Considerations.....	31
<b>Results / Discussion.....</b>	<b>33</b>
Research Organization.....	34
Plasma Optimization Results.....	35
Temperature Results.....	37
Ozone Results.....	39
Single Pass Results.....	41
Closed Loop Results.....	43
By-Product Analysis Results.....	48
Costs.....	49
<b>Conclusions / Recommendations.....</b>	<b>51</b>

<b>References.....</b>	<b>53</b>
<b>Appendix A: Thermistor Calibration Data and Psychometric Tables.....</b>	<b>55</b>
<b>Appendix B: Transformer Optimization Data.....</b>	<b>58</b>
<b>Appendix C: Temperature Test Data.....</b>	<b>61</b>
<b>Appendix D: Ozone Gas Analysis Titration Data.....</b>	<b>63</b>
<b>Appendix E: Single Pass Run Data.....</b>	<b>65</b>
<b>Appendix F: Closed Loop Test Data.....</b>	<b>77</b>

## LIST OF TABLES

Table 1: Quantitative GC Operation Temperatures.....	21
Table 2: Qualitative GC/MS Operation Temperatures.....	22
Table 3: Variac Calibration Data.....	36
Table 4: Temperature Experiment Results.....	37
Table 5: Ozone Production Conditions and Data.....	39
Table 6: Conditions and Results of Single Pass Destruction Runs.....	41
Table 7: Closed Loop, Seventeen Cycle Test Results.....	44
Table 8: Reactor By-Product Identification.....	48
Table 9: Plasma System Capital Costs.....	49

## LIST OF FIGURES

Figure 1: Picture of a Liquid Electrode Plasma Reactor.....	9
Figure 2: Plasma Reactor Cross Section.....	10
Figure 3: Picture of Working Liquid Electrode Plasma Reactor.....	11
Figure 4: Electronics Schematic.....	12
Figure 5: Thermistor Housing and Setup.....	13
Figure 6: Thermistor Calibration Chart.....	14
Figure 7: Temperature Experiment Schematic.....	16
Figure 8: Ozone Experiment Schematic.....	17
Figure 9: Single Pass System Schematic.....	18
Figure 10: Closed Loop System Schematic.....	20
Figure 11: Transformer Primary Current Curves.....	24
Figure 12: Transformer Apparent Power Curves.....	24
Figure 13: Research Process Flow Diagram.....	34
Figure 14: Plasma System Temperature versus Run Time.....	38
Figure 15: Ozone Production Rate versus Air Flow Rate.....	40
Figure 16: Destruction Efficiency versus Supplied Primary Power.....	42
Figure 17: Closed Loop, Plastic Vat Test Results.....	43
Figure 18: Closed Loop, Metal Vat Test Results.....	44
Figure 19: Closed Loop, Low Concentration Test Results.....	45
Figure 20: Closed Loop, Air Injection Test Results.....	46
Figure 21: Closed Loop, Oxygen Injection Test Results.....	46

## **Introduction**

### ***Ethylene Problem***

Fruits, vegetables, and floriculture plants are highly susceptible to postharvest deterioration before reaching the consumer. In developing countries, postharvest losses sometimes reach 75% (Marcellin, 1982). Ethylene can be a significant contributor to this quality loss.

Ethylene (C<sub>2</sub>H<sub>4</sub>) is naturally biosynthesized during the ripening of many fruits and vegetables and during flower senescence. Atmospheric ethylene, introduced by ripening fruit or other means, can precipitate or induce further ripening. By accelerating the ripening process, ethylene reduces storage life and lowers quality which can also lead to increased susceptibility to physiological diseases (Kader et al., 1985). The effects of ethylene are not all negative though. Ethylene is beneficially used in many instances such as the promotion of even ripening in bananas, degreening of fresh citrus and as an abscission agent for many crops.

Different plants and plant fruits biosynthesize different amounts of ethylene as they ripen or senesce. Normal levels of ethylene production by produce are small (< 1 ppm) and under normal conditions, no harmful effects occur (Kader et al., 1985). However, in enclosed storage facilities this natural ripening process leads to harmful build-ups of ethylene, resulting in spoiled produce and lost dollars. Different types of produce also have different sensitivities to the harmful effects of ethylene. The problems that persist with ethylene are those of adequately controlling ethylene concentration and the exposure of sensitive products to ethylene.

The postharvest storage environment that a product experiences on the farm and during the journey to the retail market can vary widely and can be dependent on the proximity of retail markets to production areas. Small producers may choose relatively local markets, have a simple chain of distribution, and thus have less stringent requirements for preserving quality due to a shorter distribution period. Conversely, larger producers, packers, shippers, and buyers must have good control over produce handling, shipping, and storage during distribution because of the longer distances and time periods required to reach the retail market. Operations at the grower/packinghouse level generally afford the best opportunities for optimized storage conditions. At this level only a single or few commodities may be handled and the large volume can justify the construction of storage environments for specific commodities and their varieties. Central collection-distribution centers, which also handle large volumes of produce, are sometimes equipped to handle single commodity storage requirements but because of the variety of produce they receive, often several hundred, management abilities and facilities become constraints.

During transportation and retail distribution many commodities may share the same storage environment and thus creating ideal storage conditions, for each, becomes difficult. The conditions within these facilities typically try to match products with similar temperature requirements and may range from 33-50°F. Temperature conditions alone may account for several different storage environments. Similarly, humidity requirements range from 85 to 100% except for a few products such as onions that require much lower humidities (Ashby et al., 1987). Optimal conditions for a product help to slow down mold

and other food spoiling agents and prevent dry rot, water loss shrinkage, or wilting (Kader et al., 1985).

While temperature and humidity are the most important factors for storage environments, the separation of products that are abundant producers of ethylene from those which are ethylene sensitive is critical. Because of the restrictions placed on the intrusion of outside air, gases such as ethylene tend to build up inside the storage facilities. Sealing the rooms, except for the various doorways through which produce enters and exits, reduces the cost of maintaining the proper environmental condition. Conventional methods of controlling ethylene have not always proved to be economical or practical under all types of storage conditions.

Storage facilities currently employ several methods of ethylene control. These methods include venting, potassium permanganate oxidation, adsorption onto brominated carbon, catalytic oxidizers, and hypobaric storage. Venting reduces ethylene concentration by bringing in outside air using an intake fan and a passive exhaust. However, venting does not sufficiently lower ethylene levels and also requires cooling outside air which leads to extra energy consumption (Pech and Latche, 1985). Potassium permanganate ( $\text{KMnO}_4$ ) oxidizes ethylene to carbon dioxide and water.  $\text{KMnO}_4$  is an effective scrubber, but its efficiency declines sharply at 90-95% relative humidity and requires continual replacement (Pech et al., 1987). Brominated carbon adsorbs ethylene from the air. However, potassium permanganate systems are cheaper and more widely available. Catalytic oxidizers, combined with ethylene and oxygen, convert the ethylene to carbon dioxide and water. However, the process requires heating the storage air to a high temperature and subsequent re-cooling (El-Blidi et al., 1993). Hypobaric (low pressure)

storage is useful in the reduction of ethylene produced by fruits, vegetables, and flowers. However, the apparatus used is cumbersome and expensive (Kader et al., 1985). These methods help to control and remove ethylene from storage facilities, but each has deficiencies for controlling large spaces or high ethylene-yield produce and can cause changes in cold and humid environmental conditions present in storage facilities. In conclusion, no system is considered ideal for ethylene control and better methods are desired.

A safe and low cost alternative technology for ethylene control is the liquid electrode plasma. Research shows plasmas work under humid conditions and also destroy gases similar to ethylene (Hurst, 1993). A plasma is a highly ionized mixture, usually gas, in which most of the particles act independently of each other. Plasma research began in the 1930s. Many people of the time believed plasma was a fourth state of matter (Glockler and Lind, 1938). However, today the scientific community accepts plasma as a different form of one of the three states of matter. Plasma research of the 1930s focused on creation of new products from simple components. The intention of this early research was to make life easier for humanity through science and technology. However, after very limited research and development and disappointing findings, the field lost support and diminished in importance. Much of the problem centered on the limited availability and control of electricity, the key to conventional plasma formation. Plasma research resurfaced in the later 1970s, sparked by more sophisticated electrical control and humanity's pressing need to clean the environment. However, unlike in the 1930s, plasma science now proceeded in reverse focusing on research to break complex products down to simple components.



## **Plasma Physics**

Throughout the universe plasmas appear in such forms as heat-induced, radiation-induced, and electrically-induced plasmas. On earth, nature produces plasma in the form of lightning bolts. These narrow strips of electricity cause ionization of the surrounding air by inducing a very intense electric field. Usually, the associated air is up to 20% ionized (Encarta, 1994). The earth's ionosphere is another example of a plasma. The glow of the aurora borealis is the visual representation of this plasma's existence. In fact, much of the composition of the universe is plasma of various forms and designs. Thermally-induced plasmas exist inside the sun and other stars, and radiation-induced plasmas exist as interstellar gases (Glockler and Lind, 1938). In any case, the plasma forms due to the acceleration of electrons independently of the particles around them. Thus, electrons behave as if they were under intense heat, in excess of 3000K, while other particles behave as if they were under normal ambient conditions.

Inside a plasma formation several reactions (Glockler and Lind, 1938) take place including:

- rebound,
- radical formation,
- higher orbital electron clusters, and
- light production.

Rebound reactions occur when an accelerated electron impacts a particle,  $M$ , and simply changes its trajectory due to lack of energy. Hence, these reactions are not significant to the destruction mechanism of a plasma reaction. Radical formation occurs when an accelerated electron impacts a particle,  $M$ , and breaks it apart into a free electron and a

free radical. The electron can then accelerate and the radical can react with other particles in the space. A higher orbital electron cluster results from an impact between an accelerated electron and a particle, M. The resulting collision supplies an outer orbital electron with energy. The outer orbital electron jumps to a higher orbital path around its nucleus. The electron cluster will then be more reactive to other particles in the space. This reaction takes place after approximately  $10^{-7}$  seconds. Finally, light results when an accelerated electron impacts a particle, M, and supplies an outer orbital electron with energy, thus inducing it to jump to a higher orbital around its nucleus. The particle lacks other particles in the space to react with and the outer shell electron falls back to its original orbit releasing energy and emitting light as a waste product. The transmission of light is the visual indication that a plasma reaction is occurring. Also, assurance of absence of dead air space in the field is made through visual accounting of no dark spaces in the plasma.

As explained, the electric field and accelerated electrons set the stage for the production of a plasma reaction. The highly reactive radicals created by accelerated electron effects drive the actual plasma reaction. Charged hydrogen, charged oxygen, and other charge imbalanced atoms and molecules are examples of these radicals. As these reactive species form, they make up the mechanism by which substances within the plasma field are broken-down or built-up. Thus, for the destruction of ethylene, accelerated electrons, combined with effects from radical formations, would collide with the ethylene and cause it to break apart and possibly reform into other products.

### ***Things Proved and To Be Proved***

Several previous experiments and observations strengthen the idea of using a plasma reaction to destroy ethylene. However, even with all of the research associated with the destruction of ethylene in a plasma field, several facts remain to confirm. First, in 1796 Dutch scientists subjected ethylene to a spark (Glockler and Lind, 1938). The spark destroyed the ethylene, but an unknown oily substance resulted. Second, plasmas produce ozone in the presence of oxygen (Parker, 1994). Ozone in large quantities may be undesirable in fruit, vegetable, and flower environments. Third, by definition, a plasma should remain at room temperature. However, this must be proven for extended running periods. Fourth, estimates must justify plasma reactors' capital and operating costs. Hurst (1993) and Yoo (1991) reported operational costs to be \$0.0081 and \$0.85 per hour, respectively, at \$0.035 per kilowatt hour for a small system. Also, research yielded favorable results with plasma reactors running at modified frequencies ( $> 60$  Hz), thus increasing the acceleration of the free electrons. Costs for frequency modifications must be proven justifiable. Finally, plasmas work even under humid environmental conditions for the destruction of certain contaminants (Hurst, 1993). These same conditions must be proven true for ethylene under maximum relative humidity.

In short, combined with the research that has already been performed, new research must meet the following list of objectives:

- Plasma operating conditions modified to optimize the frequency at which ethylene destruction occurs.

- Reactor effluent temperature monitored to ensure negligible temperature increase over long operation periods.
- Plasma reactor ozone production monitored to establish production rates and ensure controllable ozone concentrations.
- Plasma reactor effluent tested to document ethylene destruction efficiency.
- Reactor effluent tested to monitor the creation of possible ethylene destruction by-products.
- Plasma reactor ethylene destruction system assessed to determine capital and operating costs.

The remainder of this document outlines and explains the materials, methods, results, and recommendations for assessment of the previously discussed objectives.

## Materials

The materials section explains various components of each experimental setup.

## Plasma System

Figure 1 is a picture of a liquid electrode plasma reactor.

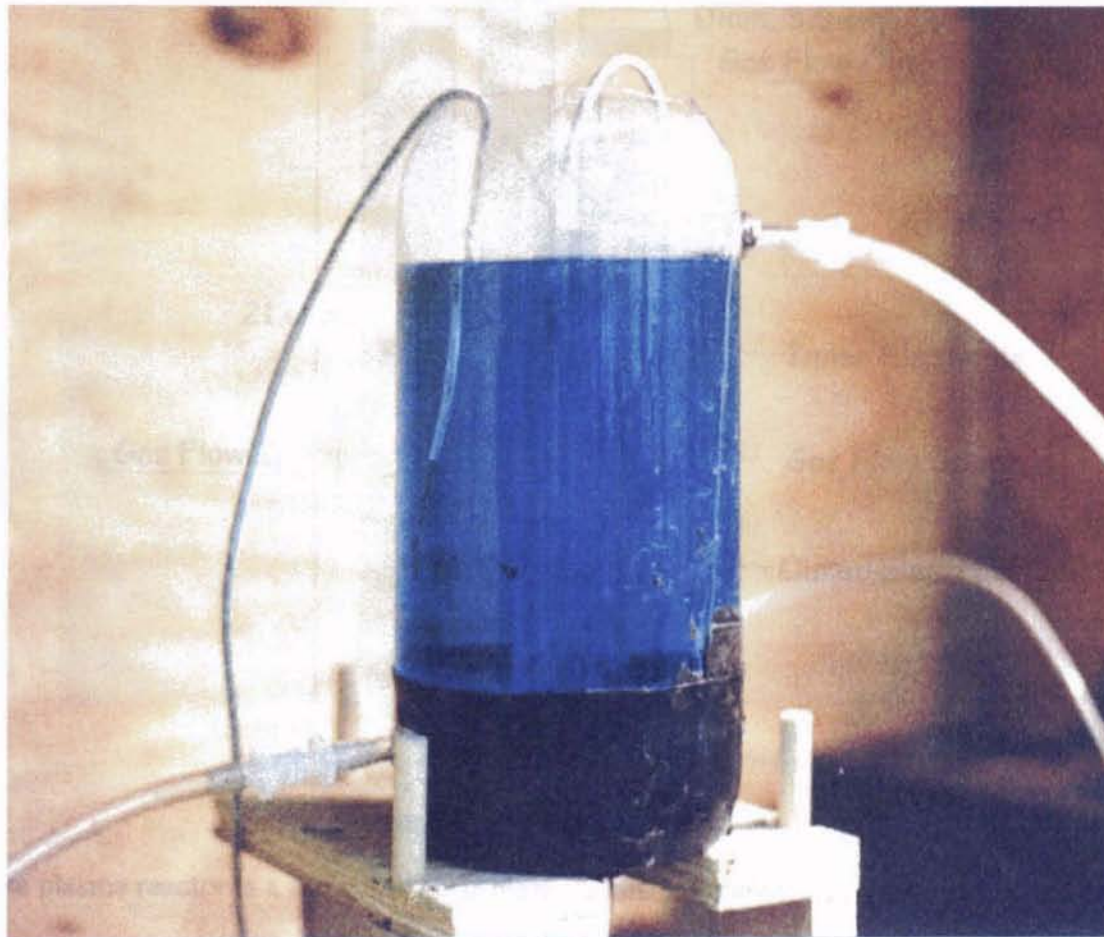


Figure 1: Picture of a Liquid Electrode Plasma Reactor

The liquid electrode plasma reactor is a relatively new form of plasma reactor. The electrodes are liquid which serve to lessen the arcing effects of flat plate plasma reactors and wire wrap plasma reactors. The setup of the plasma reactor system also serves to

allow for grounding of the outer electrode. This safety feature is beneficial in the event of an outer electrode puncture (Parker, 1994).

Figure 2 is a cross section of the plasma reactor.

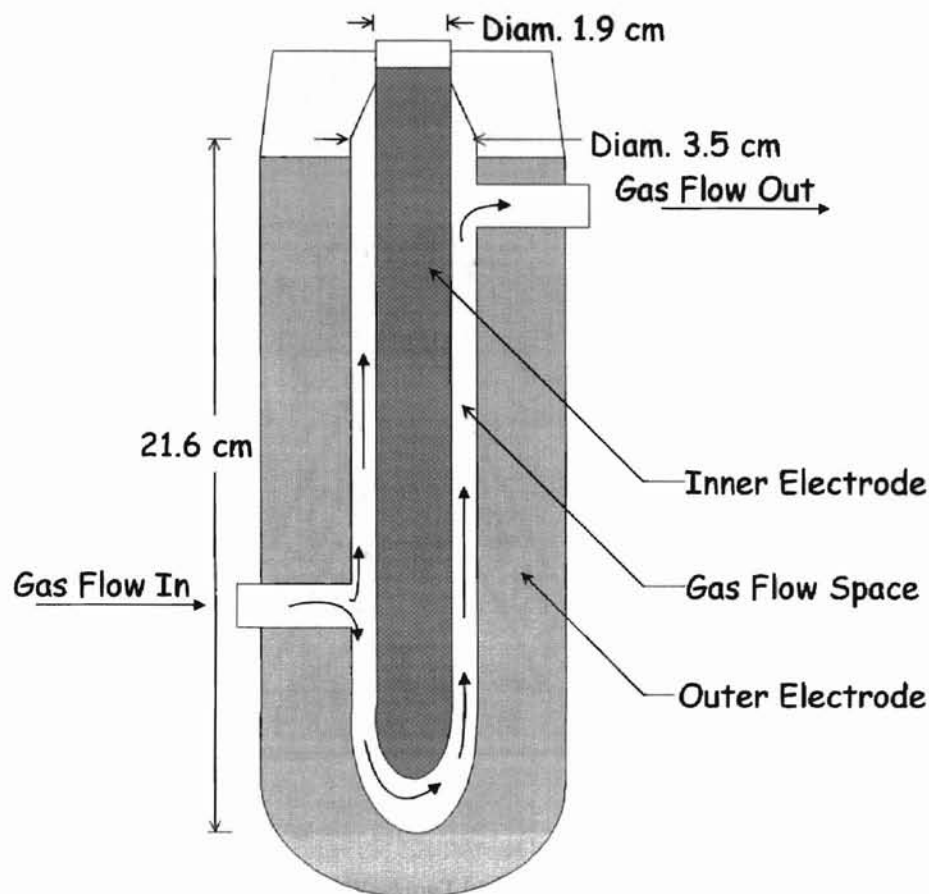


Figure 2: Plasma Reactor Cross Section

The plasma reactor is a three liter clear plastic container, making up the outside electrode, and a Pyrex glass condenser tube, making up the gas flow space and the inner electrode. The inner cylinder of the condenser tube serves as the inner electrode and the outer cylinder of the condenser tube serves as the gas flow space. The liquid filling the inner and outer electrode is a 0.013 mg/l Fisher Scientific, reagent grade, cupric sulfate and tap water solution. The cupric sulfate solution serves as the charge carrying electrode. The cupric sulfate solution serves as an ideal liquid electrode because it is non-corrosive,



conducts electricity well, and is transparent (Parker, 1994). When an alternating voltage is applied to the cupric sulfate solution, electrons accelerate in the gas flow space and a plasma field forms as shown in Figure 3.



Figure 3: Picture of Working Liquid Electrode Plasma Reactor

The plasma field is identified as the very bright vertical blue strip in the middle of the container. The dimension of the plasma field is 180.3 cubic centimeters and the gap width between the inner and outer electrodes is 0.79 centimeters.

## Electronics

In order for a plasma to be produced, electrical power must flow to the plasma reactor. Electrical connection to the frequency generator was via a normal 110 volt wall outlet as shown in Figure 4.

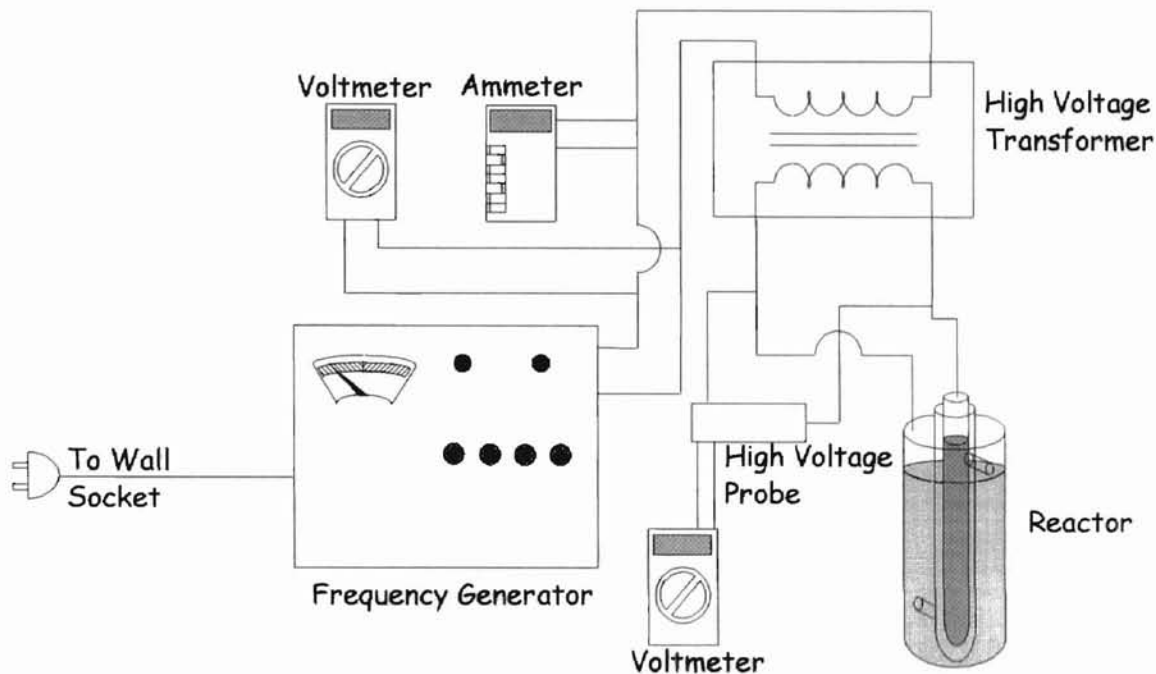


Figure 4: Electronics Schematic

The frequency generator manipulates electrical parameters with a California Instruments model 10001TC AC power source and an Invertron series 850T oscillator. The power source provides voltage control from 0 to 130 volts and the oscillator provides frequency control from 45 to 5,000 hertz. A GB model GDT-190A voltmeter, frequency oscillator, and GB model GDT-190A ammeter monitor the voltage, frequency, and amperage. The voltage and the amperage supplied to the reactor determine its power and provide an indication of the cost to operate the system. Modified voltage and frequency output from the oscillator is connected to a high-voltage France-former gaseous tube transformer. The



transformer amplifies the voltage sent to the plasma reactor. This particular transformer rates at 15,000 volts from its secondary (leading to the reactor) side. A Fluke model 80K high voltage probe, in conjunction with a voltmeter, determined the secondary voltage. Two 18-inch, 3-gauge wound copper wires carried electricity from the secondary side of the transformer to the inner and outer electrodes of the plasma unit.

### ***Thermistors***

Several experimental setups make reference to the use of thermistors. Thermistors measured the wet and dry bulb air stream temperatures. Figure 5 shows the setup of a thermistor system.

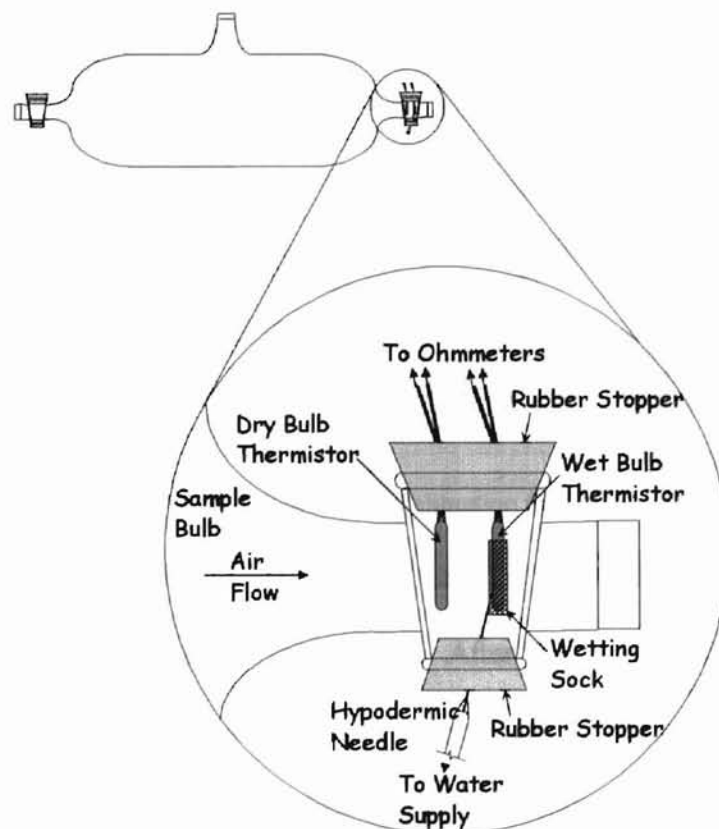


Figure 5: Thermistor Housing and Setup

The housing for the system is in place of the stopcock on a 250 ml glass sampling bulb. The thermistor housing uses two thermistors that protrude through a rubber stopper and are aligned perpendicular to the direction of air flow. A wetting sock wraps around the trailing thermistor that will act as a wet bulb probe. A hypodermic needle contacts the wetting sock through the bottom rubber stopper. Water provided through the needle saturates the wetting sock and flows onto the thermistor.

Air temperature determines the electrical resistance across the first thermistor's tip and this resistance corresponds to a temperature found on a thermistor calibration chart as shown in Figure 6.

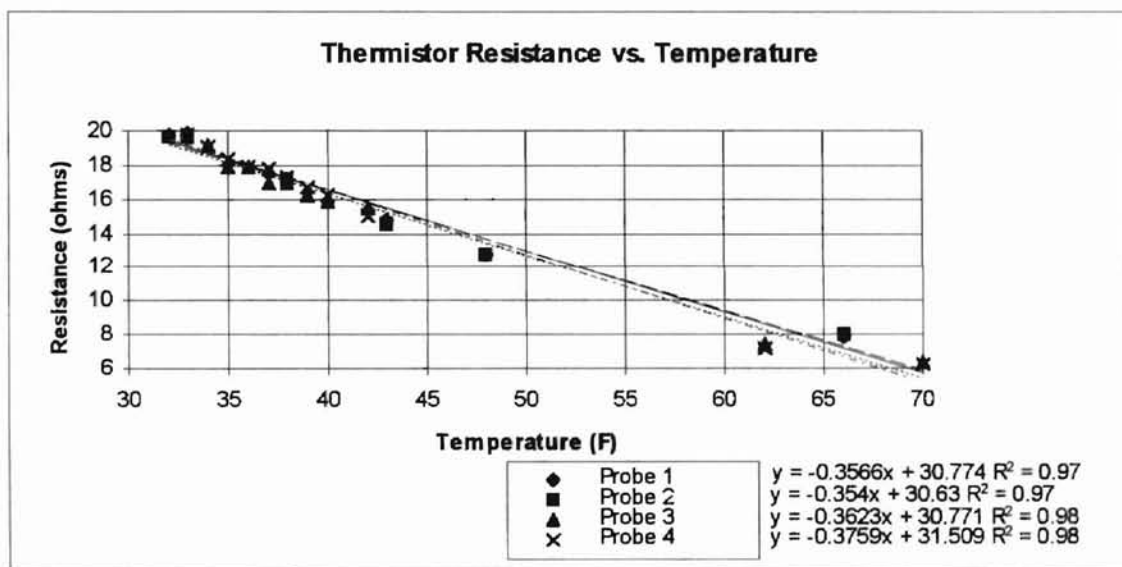


Figure 6: Thermistor Calibration Chart

Thermistor calibration was achieved by placing them in water at various temperatures and recording the associated resistance (Appendix A). After plotting the thermistor resistance versus temperature, a least-squares analysis determined the calibration equation for each probe. Throughout all experiments, probes 1 and 2 were coupled into one thermistor

setup with probe 2 acting as the wet bulb. The same holds true for probes 3 and 4 with probe 4 acting as the wet bulb.

The second (trailing) thermistor also produces a resistance proportional to thermistor temperature. The thermistor's resistance in this case is proportional to the wet bulb temperature. Using the calibration chart and a psychometric table (Appendix A) the relative humidity of the air stream was determined from the dry and wet bulb air temperatures.

### ***Other Common Elements***

For all experimental setups, quarter inch Tygon tubing with an inert Teflon inner lining was used. In places where tubing could not be used, quarter inch stainless steel tubing was used instead. Both of these products were used to assure no reaction occurred between the tubing and ethylene or any plasma reactor produced by-product.

The flow meters used in every experiment were five liter-per-minute calibrated Bendix flow meters. They operated by suspending a small steel shot in a gas stream.

The sampling bulbs used were 250 ml Fischerbrand Septum-Port Gas Sampling Tubes made with Pyrex glass. Glass stopcocks or the previously discussed thermistor setup equipped each end of the bulbs. The sampling bulbs also contained a rubber/Teflon sampling septum.

## Temperature System

To provide information on temperature effects of a working plasma on the air that passed through it, a setup such as the one shown in Figure 7 ran air through the reactor.

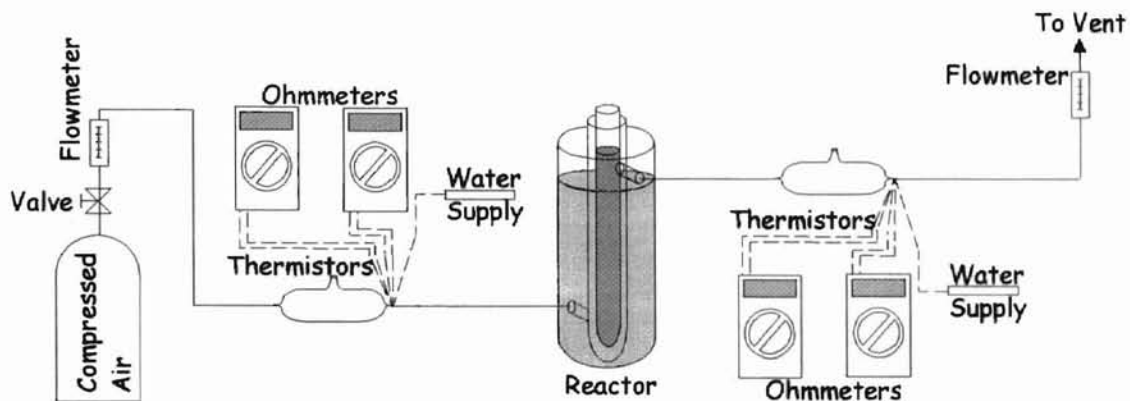


Figure 7: Temperature Experiment Schematic

From the compressed air tank, dry-grade air ran at 3 l/min through a flow meter, to a set of thermistors, through the reactor, to another set of thermistors, through another flow meter, and finally to a fume hood vent. The thermistors monitored the temperature of the influent and effluent air streams. Line lengths between all major components were less than 16 inches. The entire setup was also insulated with quarter inch pipe wrap to help lessen the effects of any heat loads or heat drains being imposed by the environment.

## Ozone System

Since ozone is a known by-product of plasma reactions with oxygen (Glockler and Lind, 1938), and concentrated ozone is potentially harmful to produce, a set of ozone production experiments ensued. Figure 8 shows the setup for the ozone production experiments.

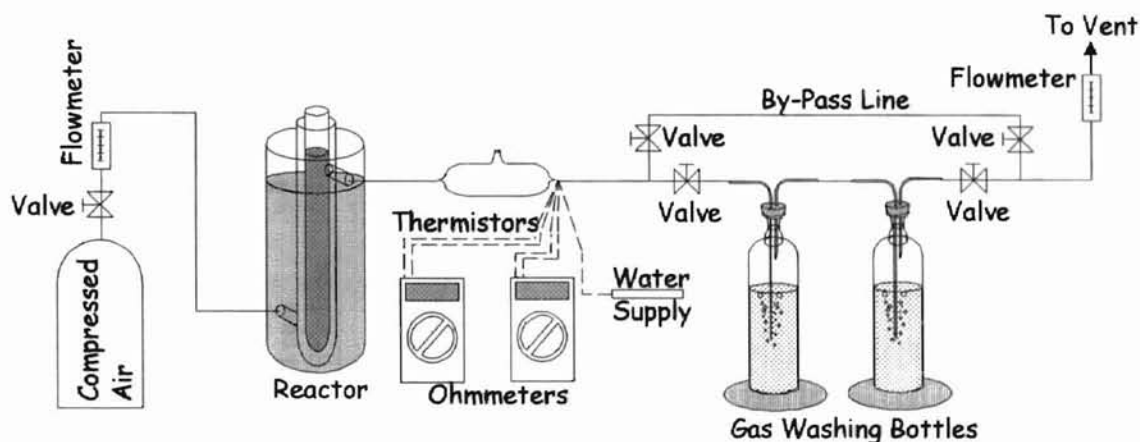


Figure 8: Ozone Experiment Schematic

From a compressed air tank, dry-grade air ran at from 1 to 5 l/min through a flow meter, through the reactor, to a set of thermistors, to a tee in the line, and finally through another flow meter and to a fume hood vent. At the tee in the line were two 1000 ml Pyrex, glass gas washing bottles with an optional by-pass line. A 0.05N potassium iodine solution filled the gas washing bottles for titrimetrically determining the concentration of ozone in the reactor effluent. The methods section further details the ozone concentration determination process.

## Single Pass System

Research involving the destruction efficiency of ethylene inside a plasma reactor used the setup in Figure 9.

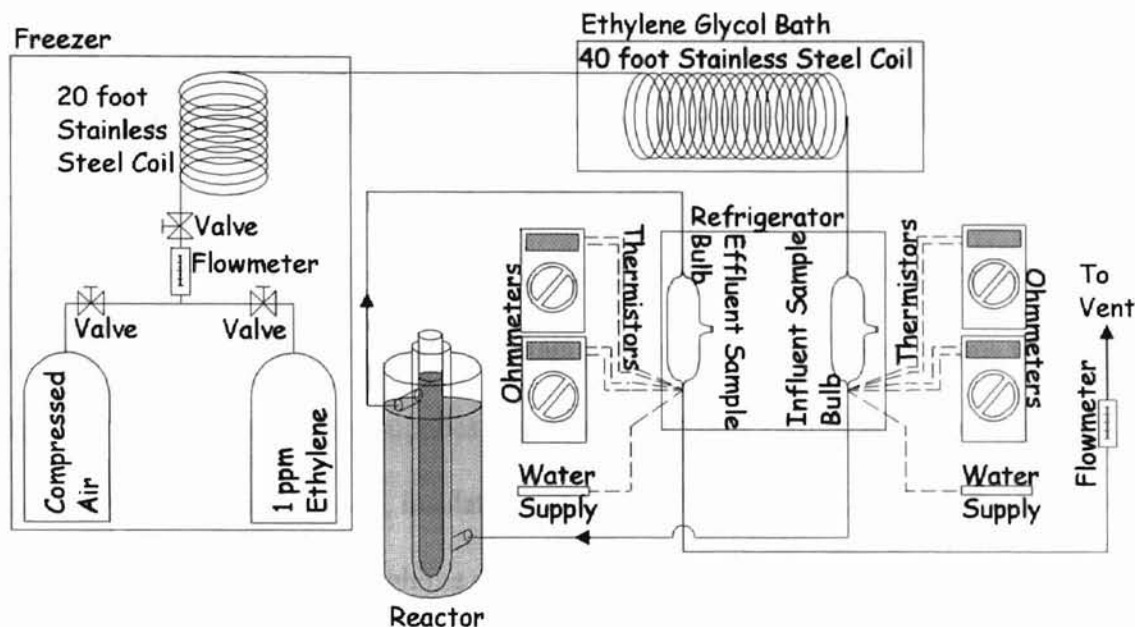


Figure 9: Single Pass System Schematic

In order to simulate conditions of temperature and humidity inside a produce storage warehouse the entire process ran through a series of chilling units. The first chilling unit was a 25 cubic foot Signature freezer. Dry-grade air ran through the system for 20 minutes at the beginning of each test to bring it to thermodynamic equilibrium. Ethylene at 1 ppm, balanced in air, was then run through a flow meter and then through a 20 foot, half inch stainless steel coil for additional cooling. Ethylene stored in the freezer only reached 55°F because of cooling limitations implied on a pressurized gas. After the first coil a second, 40 foot, half inch stainless steel coil was submerged in a 15 gallon Precision low temperature bath of ethylene glycol maintained at 10°F. The one foot of tubing reaching from the freezer to the bath was heavily insulated with quarter inch pipe wrap to

decrease thermal loads. The residence time inside the ethylene glycol bath allowed the ethylene to reach a temperature below the desired 50°F run temperature. Also, as the gas reached this temperature it passed below its dew point bringing its humidity above the desired 90% run humidity. From the second coil, the ethylene passed through the influent sampling bulb and on to the first set of thermistors. After the thermistors the ethylene ran through the plasma reactor and then back through the effluent sampling bulb, to a second set of thermistors, through a second flow meter, and to a fume hood vent. Both sampling bulbs and thermistors were chilled inside a 2 cubic foot General Electric refrigerator. The refrigerator remained at 33°F to help maintain proper environmental conditions while not allowing the thermistor water supplies to freeze. The entire refrigerator assembly was attached to a piece of plywood, insulated and mounted on the front of the refrigerator in place of the door. Holes through the plywood for sampling septums provided access to sampling bulbs. The thermistor connections and syringes also extended outside the refrigerator. All of the tubing connecting the various main processes was insulated with quarter inch pipe wrap. The lengths from the bath to the refrigerator, the influent side of the refrigerator to the plasma reactor, and the plasma reactor to the effluent side of the refrigerator, were one foot, four feet, and four feet, respectively.

### ***Closed Loop System***

In order to further mimic conditions of a produce warehouse, ethylene destruction also occurred inside a closed loop system. The closed loop system ran under ambient room temperatures (65°F to 70°F) and humidities (20%-40%) within a 24 liter system.

The purpose of running under these conditions was to determine the effects of allowing ethylene to pass through a plasma reactor several times. Figure 10 illustrates the setup of the closed loop system.

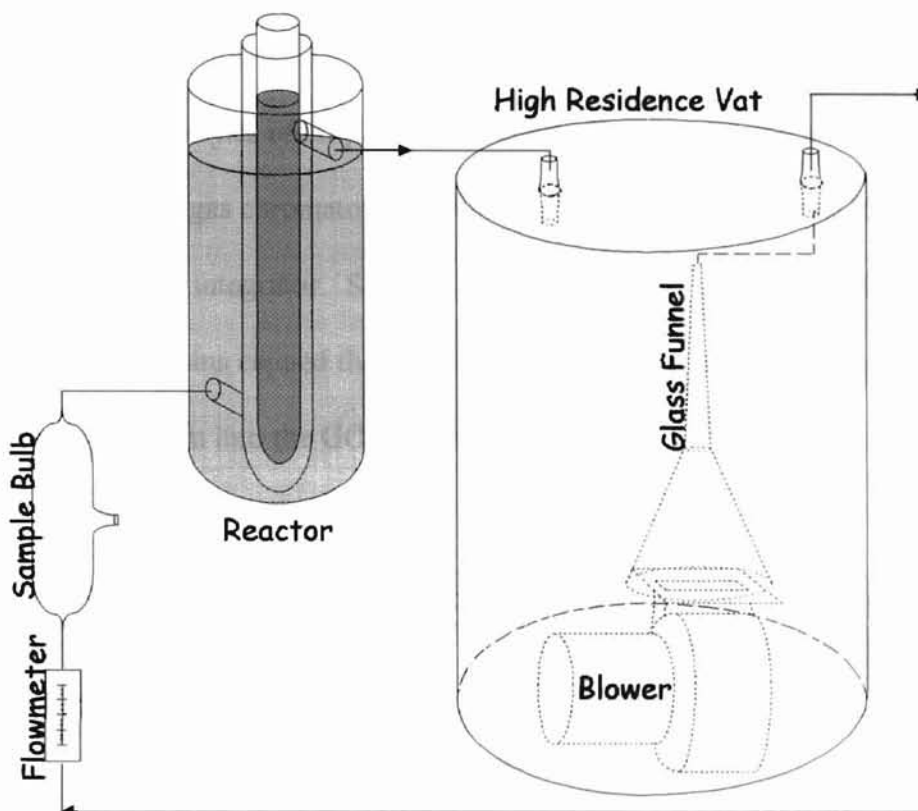


Figure 10: Closed Loop System Schematic

The 23 liter high residence vat simulates the large open space inside a produce warehouse. Inside the vat is a Dayton type U21B blower connected to a glass funnel. The blower pulls the air-ethylene mixture from the bottom of the vat up through the funnel and out of the vat. With this arrangement a constant circulation occurred inside the vat and no dead air spaces diminished the blower's efficiency. From the vat the ethylene travels through a flow meter, sampling bulb, and to the reactor. After passing through the reactor, ethylene then travels back to the vat to restart the loop. The volume of the loop outside the vat is



approximately 1 liter, bringing the total system volume to 24 liters. The blower was able to run the system at a flow rate of 1 liter/minute allowing for a 24-minute cycle.

### ***Analysis Equipment***

Quantitative analysis of ethylene destruction efficiency utilized a Tracor Instruments Model 540 gas chromatograph (GC) combined with a Spectra-Physics 4270 graphical and numerical integrator. Sampling occurred using 3 ml gas-tight Teflon syringes. Surgical septums capped the ends of the syringe needles after taking samples and before injecting them into the GC. Table 1 gives a list of pertinent quantitative GC component temperatures.

<b>Variable</b>	<b>Setting</b>
Oven Temperature	60°C
Injector Temperature	180°C
Detector Temperature	200°C

Table 1: Quantitative GC Operation Temperatures

The GC analysis was an isothermal process using a 30-meter J&W Scientific GS-Q Megabore column with a 0.53 mm inner diameter and porous divinyl benzene homopolymer, porous layer open tubular phase. The GC used helium at a flow rate of 97 cm<sup>3</sup>/s as a carrier gas and a flame ionization detector (FID) to capture and analyze ethylene concentrations. The GC make-up gas was air and nitrogen.

Qualitative analysis on the plasma reactor / ethylene destruction produced by-product utilized a summa canister (USEPA's: Compendium Method TO-14, 1988) to cryogenically separate gas components. This method also produced a quantitative analysis of the by-products produced. The analysis followed the methods outlined in the USEPA's

“Compendium of Methods for the Determination of Toxic Organic Compounds in Ambient Air,” document number EPA-600/4-84-041. Qualitative analysis utilized a Hewlett Packard model 5972 gas chromatograph/mass spectrometer (GC/MS) combined with a Hewlett Packard Target System graphical and numerical integrator. Sampling occurred with a 3 liter pre-evacuated summa canister. Table 2 gives a list of pertinent qualitative GC component temperatures.

Variable	Setting
Oven Temperature	35°C-220°C
Injector Temperature	200°C
Detector Temperature	250°C

Table 2: Qualitative GC/MS Operation Temperatures

The GC/MS analysis was a non-isothermal process running at 35°C for 1 minute, ramping at 10°C/min to 160°C, 20°C/min to 220°C, and holding for 5 minutes at 220°C. The process used a 60-meter J&W Scientific DB5 column with a 0.35 mm inner diameter and 5% phenyl-methyl polysiloxane stationary phase. The GC used helium at a flow rate of 1 ml/sec as a carrier gas with no make-up gas.

## Methods

This section explains the experimental procedures used both to prepare for and perform data collection.

### *Plasma Optimization*

A series of transformer curves defined the most efficient plasma operating conditions. Plasma optimization used the following experimental methods:

- Setting the frequency generator to 50 hertz
- Increasing the primary voltage until a plasma began to form
- Recording the amperage while increasing the voltage in 10-volt increments until 120 volts was reached or until the plasma began to arc from one of the electrodes
- Lowering the voltage until the plasma was no longer visible
- Repeating the above steps while increasing the frequency in 10-hertz increments from 50 to 260 hertz, 20-hertz increments from 260 to 600 hertz, and 50-hertz increments from 600 to 700 hertz

Figure 11 illustrates the family of curves generated from the recorded data located in Appendix B.

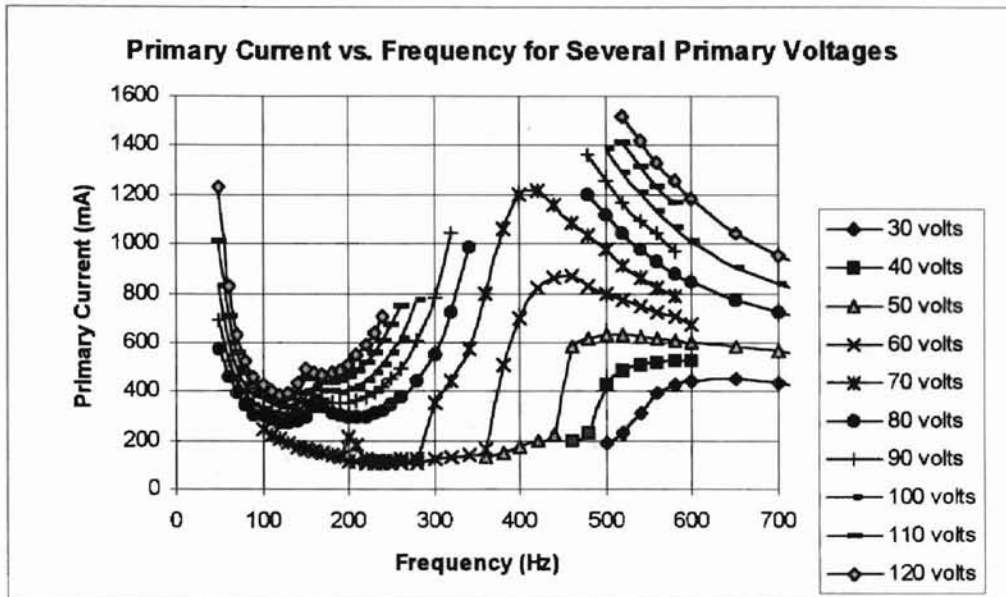


Figure 11: Transformer Primary Current Curves

The points at which a curve stops and then restarts indicates an area where the plasma unit was beginning to arc across electrodes and short out due to energy overload. These missing curve points are areas in which the transformer is susceptible to exceeding its secondary voltage limit of 15,000 volts.

Multiplying the amperage by the voltage generated a set of apparent power curves for the transformer. These curves determined the optimum plasma operating condition. Figure 12 shows the results of the power curves.

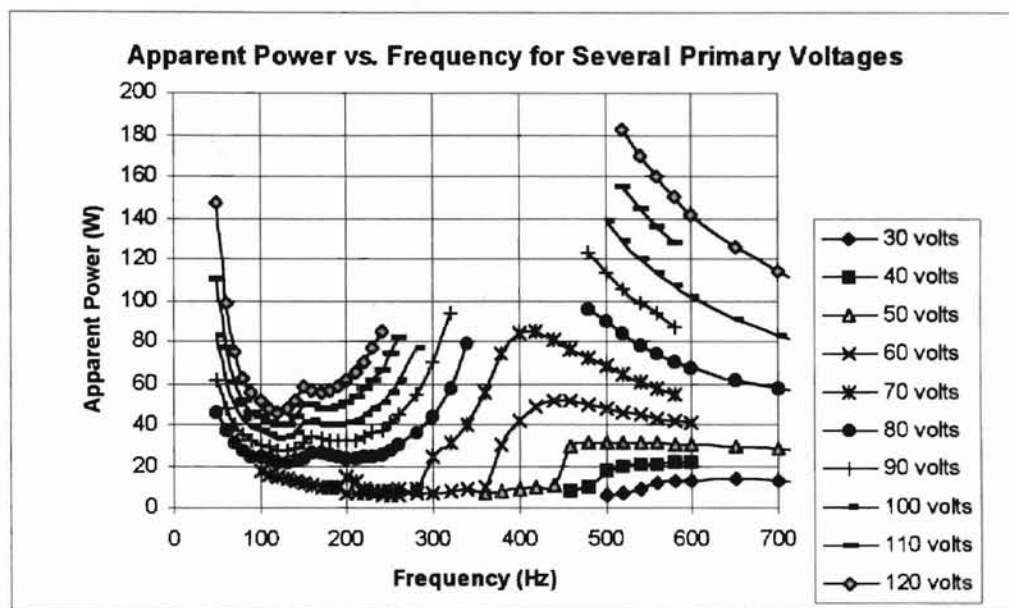


Figure 12: Transformer Apparent Power Curves

The apparent power actually has units of volt-amperes due to the theoretical capacitance associated with the load pulled by the plasma reactor. This load combines capacitance and resistance and results in a power unit of volt-amperes, however the standard power unit of watts will be used throughout this document for ease of notation and understanding.

Each transformer requires a different set of power curves due to slight variations in design and construction. However, all curves follow the same “humped” trend dictated by the hysteresis of the transformer’s electrical behavior. Typically, the most efficient region of the power curve falls at a high power and low frequency. For this particular transformer that region occurs around the 60-hertz range. This 60-hertz value is also the frequency generated from a normal wall socket. Therefore, most ethylene destruction tests ran at 60 hertz and varying primary voltages from 95 to 126 volts, creating a range of

power from 54 to 115 watts. Also, ethylene destruction tests ran at 440 hertz with 56 volts and 40 watts of power to determine the effects of a higher frequency on efficiency of ethylene destruction in the plasma reactor.

### ***Temperature Experiments***

A temperature experiment determined the effects of a working plasma on air stream influent and effluent temperature differential. This experiment ensured that electrons in the plasma unit actually act independently of other particles around them as per the definition of a plasma field. After setting up the temperature system, according to the previously mentioned schematic, the experimental procedure ran as follows:

- Turning on air at 3 l/min
- Adjusting the operating conditions to achieve a 12.5 kV secondary voltage
- Running the system for 12 hours
- Monitoring influent thermistor, effluent thermistor, inner electrode temperature, and outer electrode temperature at various intervals
- Shutting down air and plasma

Data from the temperature experiment (Appendix C) determined an estimated equation for the effects of the working plasma on the effluent stream. This equation, in turn, optimizes plasma run time in produce warehouses in order to balance ethylene destruction need with electricity costs.

## Ozone Experiments

Ozone production experiments determined the concentration of ozone produced by the plasma reactor. Since high levels of ozone ( $O_3$ ) harm produce, the experiment required a conservative estimate of ozone production. To achieve a conservative estimate, dry-grade air ran in the experiments. Ozone production is dependent on the oxygen concentration. Therefore, the air simulated a condition in the warehouse for which no ethylene or other contaminant was present and the plasma reactor was in operation with pure air. The testing procedure followed the format below:

- Setting up according to schematic
- Filling gas washing bottles with 500 ml each of 0.05N potassium iodide
- Turning on air to 1, 3, or 5 l/min
- Turning on plasma to 11 kV or 13.5 kV of secondary voltage
- Allowing one system volume to flow through the plasma reactor
- Attaching gas washing bottles to the effluent line
- Detaching the plasma effluent line from gas washing bottles when the first bottle is a deep yellow and the second bottle begins to turn yellow
- Shutting down air and plasma
- Performing ozone titration experiment on contents of gas washing bottles according to "Ozone Gas Analysis: Iodometric, Wet Test Method" method number 422 as outlined in Appendix D (APHA et al., 1980)
- Monitoring total gas washing run time and ozone production amount to determine final ozone production rate under given conditions

The Ozone Gas Analysis: Iodometric, Wet Test Method involves the titration of partially ozone saturated 0.05N potassium iodide (KI) with 0.05N sodium thiosulfate ( $\text{Na}_2\text{S}_2\text{O}_3$ ).

Calculation of the ozone concentration follows the equation:

$$\text{mg/l O}_3 = (\text{ml of Na}_2\text{S}_2\text{O}_3 \times \text{Normality of Na}_2\text{S}_2\text{O}_3 \times 24,000) / \text{ml of gas sampled},$$

where 24,000 serves as a conversion factor to convert the final answer into units of mg/l.

### ***Single Pass Ethylene Destruction Experiments***

Single pass ethylene destruction tests determined the efficiency of the plasma reactor in ethylene destruction. The experimental method used the following list of steps:

- Setting up according to the schematic described in the materials section
- Pre-chilling the freezer, refrigerator, and water bath
- Turning on ethylene to 1, 3, or 5 l/min
- Turning on plasma to desired secondary voltage, primary voltage, and frequency
- Taking separate influent and effluent 3 ml syringe samples at defined time intervals
- Monitoring influent and effluent temperature and humidity
- Shutting off ethylene and plasma unit
- Testing ethylene concentration of sample syringes on GC unit

Due to time delays between taking samples and running them on the GC unit, each syringe remained in a holder with its needle inserted into a septum to prevent gas leakage.

Conversations with a researcher in the horticulture field (Anderson, 1996) and resulting



lab effluent data of approximately 1 ppm indicate time delays between sampling and testing on the order of these experiments (1-2 hours) had no adverse effects on sample quality. Effluent samples were from a 1 ppm compressed ethylene tank used as a standard for calibration.

### ***Closed Loop Ethylene Destruction Experiments***

A closed loop system simulated enclosed conditions of a produce warehouse. Experiments determined the effects of multiple passes of an ethylene stream through the plasma reactor. The closed loop experiments used the following procedure:

- Setting up according to the closed loop schematic detailed in the materials section
- Pre-exposure of the system by allowing one system volume of ethylene to circulate
- Closing system and allowing system to set for 24 hours
- Running three system volumes of ethylene through the system and resealing the system
- Turning on the blower to begin ethylene circulation
- Turning on the plasma to the desired secondary voltage, primary voltage, and frequency
- Monitoring the run time and taking 3 ml syringe samples of the re-circulating flow at allotted times
- Turning off the blower and the plasma unit

- Testing concentrations of ethylene in syringe samples on the GC unit

The system soaked in a 1 ppm ethylene-air mixture for 24 hours to minimize any ethylene adsorption by system components during the experiments. As with single loop experiments, the sample-containing syringes remained in a holder and a septum to prevent leakage.

### ***By-Product Identification Experiment***

The closed loop system also served as an ideal collection basin for the purpose of taking a summa canister sample (USEPA's: Compendium Method TO-14, 1988) of the plasma reactor by-product(s). The by-product identification experiment used the following procedure:

- Setting up according to the closed loop schematic detailed in the materials section
- Pre-exposure of the system by allowing one system volume of ethylene to circulate
- Closing system and allowing system to set for 24 hours
- Running three system volumes of ethylene through the system and resealing the system
- Turning on the blower to begin ethylene circulation
- Turning on the plasma to the desired secondary voltage, primary voltage, and frequency

- Monitoring the run time and using the summa canister to remove the gas contents of the high residence vat
- Turning off the blower and the plasma unit
- Identifying the plasma reactor / ethylene destruction by-product using cryogenic freezing and a GC/MS (mass spectrometer) unit

### ***Special Considerations***

The design of the special considerations section is to help those attempting to recreate the previously discussed experiments. The advice given here came about through the trial and error process. The following list includes some research hints.

1. Condensation on the inside of the plasma reactor unit results in the “spider web” effect. The spider web effect occurs as condensing water droplets cause arcing inside the unit and partially short out the plasma field. Condensation results when the liquid electrode temperatures are less than the dew point temperature of the influent gas.
2. Use of a cold room to simulate temperature conditions inside a produce storage warehouse promotes the above mentioned spider web effect. A compressed gas cannot quickly reach the desired 50°F temperature due to the energy required to chill a compressed gas. Therefore, the gas must travel through a pre-chiller, such as an ethylene glycol bath, to ensure it reaches the desired temperature.

3. The thermistors, used to monitor humidity, were difficult to use. Over-saturation of the wetting sock led to inaccurate readings and the water supply froze easily under the chilled conditions.
4. Creation of an air stripping tower, used to add humidity to the system, added several weeks to the research. The psychometric charts (Appendix A) show that the air-ethylene mixture reaches its dew point temperature around 50°F. This can be found in Table A of Appendix A by reading the tank effluent gas temperature of 55°F and the wet-bulb thermistor depression of 3°F. The result is a 50°F dew-point temperature. Therefore, chilling the mixture below its dew point ensures a relative humidity greater than 90%, requiring no stripping tower.
5. At high voltages generated on the secondary side of the transformer, a skimming effect occurred on the high voltage probe lead wires. This skimming effect is the result of leads being too small to handle applied voltages. The effect is visible as wires glow when the research room is dark and the plasma unit is running. To solve the problem lead wires were wrapped in Tygon tubing and electrical tape to increase their insulation.
6. As wire leads connecting the plasma unit to the transformer sat in their respective electrodes, they exhibited a capillary effect with the electrode cupric sulfate solution. This caused corrosion to occur on transformer terminals and had potentially hazardous consequences as a pool of liquid formed at the transformer base. The best solution to the problem involved removing wires from the liquid electrodes between uses.

## **Results / Discussion**

### ***Research Organization***

As with every multiphase research-oriented project, details of each experiment sometimes mask the overall process flow. Often, to properly answer questions stated by the experimental objectives requires several groups of related experiments. Therefore, to help the reader understand the overall design of this research, Figure 13 presents a process flow diagram outlining the different research phases along with each phase's sub-experiments.

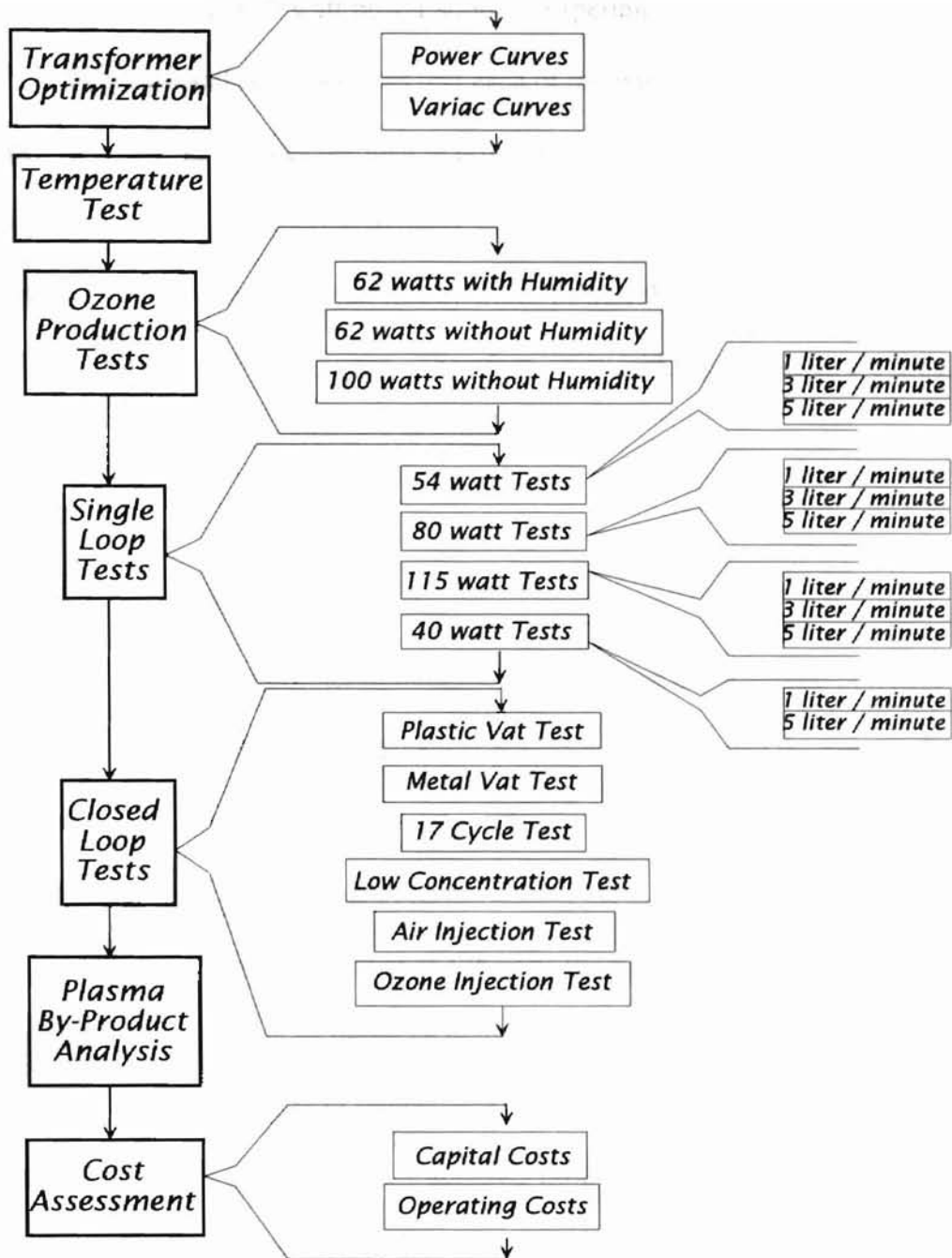


Figure 13: Research Process Flow Diagram

The left-hand column of Figure 13 represents the major objectives of the research. The middle column and the right-hand column each represent subdivisions of experiments required to meet the objectives. For example, the single loop tests answered questions for the fourth objective of determining plasma reactor ethylene destruction efficiency. Tests

included 54, 80, 115, and 40 watt power supplied experiments, as indicated by the middle column. The right-hand column shows that each of these four experiments divided into subexperiments of various liter per minute flow rates. At this point it is important to reiterate that even though different frequencies are discussed during transformer optimization tests, they are only vehicles by which power, the ultimate measurement of transformer performance, is delivered. Therefore, no specified frequencies are used to designate the single loop experiments or subexperiments.

### ***Plasma Optimization Results***

Plasma system transformer optimization met the first experimental objective. Optimization consisted of running a family of power curves to define the points of maximum plasma run efficiency. As shown in the methods section, the point of optimization (most efficient) power occurred around the 60-hertz curve section. The transformer provided maximum power at 126 volts (primary voltage), creating 115 watts of power, at 60 hertz, within its optimum range. Although this result is only significant for this particular transformer, due to transformer variance, it is quite fortunate. A 60-hertz frequency corresponds to the frequency available through a typical wall socket. Therefore, for industrial application a simple Variac replaces the frequency generator in the system setup.

A Variac controls the amount of voltage supplied to the primary side of the transformer. Table 3 shows Variac calibration data.

Variac Setting	Primary Voltage (volts)	Current (mA)	Power (W)	Secondary Voltage (volts)
7	10	95	0.95	1213
9	15	125	1.88	1806
11	20	153	3.06	2350
15	25	177	4.43	2900
18	30	203	6.09	3470
20	35	230	8.05	4020
23	40	256	10.24	4710
26	45	280	12.60	5240
29	50	311	15.55	5920
31	55	335	18.43	6400
34	60	361	21.66	7030
36	65	387	25.16	7650
39	70	414	28.98	8210
41	75	446	33.45	8720
44	80	475	38.00	9303
46	85	508	43.18	9790
49	90	536	48.24	10280
51	95	576	54.72	11070
53	100	611	61.10	11430
56	105	656	68.88	12090
58	110	707	77.77	12220
61	115	770	88.55	13000
64	120	823	98.76	13180
66	125	900	112.50	13970
69	130	1000	130.00	14600
70	135	1046	141.21	14980

Table 3: Variac Calibration Data

Note, the Variac calibration shows the amounts of primary and secondary voltage supplied to and by the transformer. As with the transformer, each Variac generates a different data set and requires individual calibration.



## Temperature Results

A temperature test met the second experimental objective. The test followed the setup and method discussed previously. The temperature test was 700 minutes in duration. Table 4 shows the resulting data.

Elapsed Time (min.)	Effluent Temperature (°F)	Influent Temperature (°F)	Inner Electrode Temperature (°F)	Outer Electrode Temperature (°F)
0	69.0	66.8	66	72
7	69.1	66.9	70	72
12	69.1	66.9	71	72
17	69.1	67.0	72	72
22	69.1	67.0	73	73
27	69.1	67.0	74	73
32	69.2	67.1	75	73
62	69.3	67.2	80	73
182	69.6	67.7	81	74
229	69.5	67.8	81	74
345	69.8	68.0	82	75
435	69.8	68.1	82	75
486	69.9	68.2	84	76
579	69.7	68.1	85	77
700	69.9	68.1	85	77

Table 4: Temperature Experiment Results

Thermometers and thermistors monitored inner and outer electrode temperatures along with influent and effluent air temperatures. Air at ambient room temperature ran through the process. The data show a 19°F rise in inner electrode temperature and a 5°F rise in outer electrode temperature. The data also show a sharp initial rise in temperature for the inner electrode. This effect occurs until the 70-minute reading at which point the temperature increases level off. This seems to be an explainable effect considering the volume difference between the two electrodes. The outer electrode is 42 times the volume

of the inner electrode and also better able to dissipate heat to its surroundings due to its location. This would also help the outer electrode resist drastic temperature fluctuations.

For the air stream temperature readings the effluent temperature consistently read a few degrees warmer than the influent temperature. However, no significant air stream temperature increase is visible with time. Figure 14 illustrates the respective temperature data points.

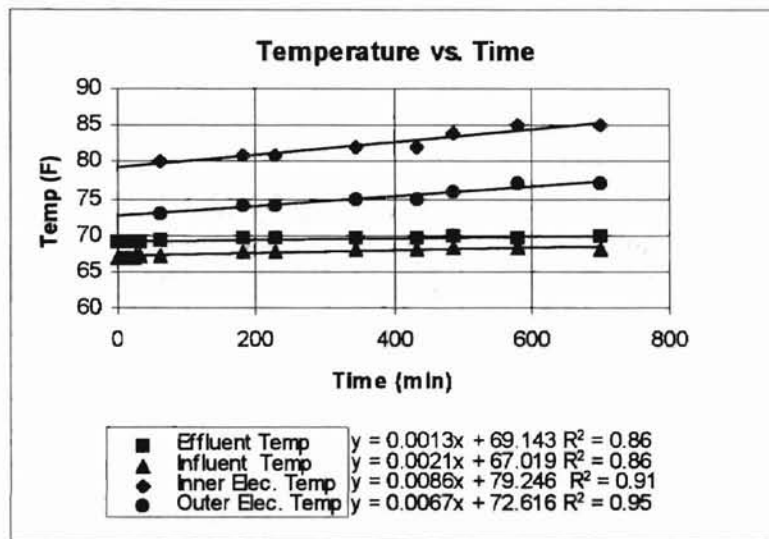


Figure 14: Plasma System Temperature versus Run Time

A least-squares fitting approach defined the temperature increase equation lines. The slope of the line indicates the degrees per minute of temperature change. However, for inner and outer electrode temperature equations, only points after the 70-minute equilibrium were used to determine the line slopes. Figure 14 indicates the effluent air stream increased 0.0013 °F/minute, which converts to 1.87 °F/day. Therefore, for a plasma system in an industrial setting, temperature effects would be negligible. A working scenario would put a system running when ethylene built up to some trigger concentration. Then, when the ethylene level dropped back to an acceptable point, the plasma would shut off and return to room temperature. A plasma unit would probably never run for 700 min

of the inner electrode and also better able to dissipate heat to its surroundings due to its location. This would also help the outer electrode resist drastic temperature fluctuations.

For the air stream temperature readings the effluent temperature consistently read a few degrees warmer than the influent temperature. However, no significant air stream temperature increase is visible with time. Figure 14 illustrates the respective temperature data points.

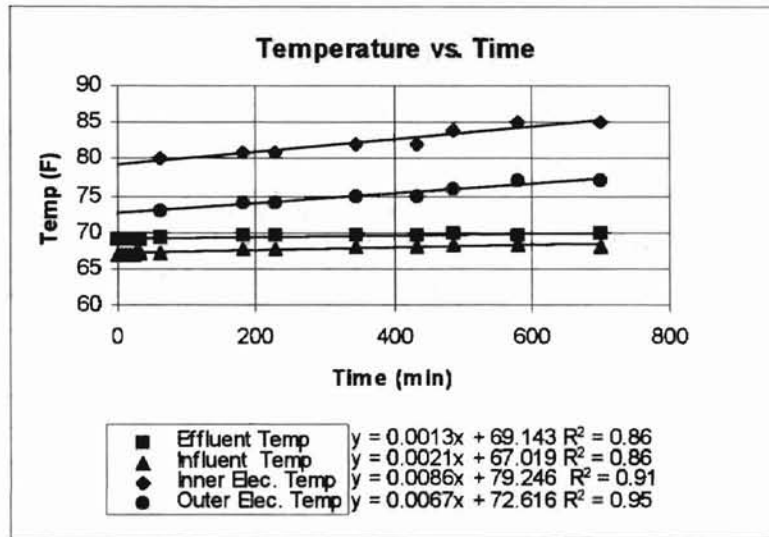


Figure 14: Plasma System Temperature versus Run Time

A least-squares fitting approach defined the temperature increase equation lines. The slope of the line indicates the degrees per minute of temperature change. However, for inner and outer electrode temperature equations, only points after the 70-minute equilibrium were used to determine the line slopes. Figure 14 indicates the effluent air stream increased 0.0013 °F/minute, which converts to 1.87 °F/day. Therefore, for a plasma system in an industrial setting, temperature effects would be negligible. A working scenario would put a system running when ethylene built up to some trigger concentration. Then, when the ethylene level dropped back to an acceptable point, the plasma would shut off and return to room temperature. A plasma unit would probably never run for 700 min

straight. Also, given the grounded properties of the outer electrode, the liquid could potentially re-circulate through a cooling bath.

### **Ozone Results**

A group of ozone production experiments for the plasma reactor met the third objective of the research. In order to get a conservative estimate, standard dry-grade air ran through the reactor. Table 5 shows the experimental criteria and the resulting ozone production rates.

Run No.	Flow Rate (l/min)	Run Time (min)	Relative Humidity (%)	Primary Power (watts)	Ozone Concentration (mg/l)	Ozone Production Rate (mg/min)
1	5	5.0	60	62	0.60	2.98
2	3	5.0	60	62	0.60	1.80
3	1	9.0	60	62	1.05	1.05
4	1	8.0	21	62	3.02	3.02
5	2	3.0	21	62	1.92	3.84
6	3	2.0	21	62	1.04	3.12
7	5	2.0	21	62	0.70	3.48
8	3	2.0	21	62	1.02	3.06
9	1	5.0	21	62	2.98	2.98
10	5	2.5	21	100	0.87	4.35
11	3	4.0	21	100	1.38	4.14
12	1	4.5	21	100	4.05	4.05

Table 5: Ozone Production Conditions and Data

The first three experiments ran at 62 watts with a relative humidity of 60% introduced into the air stream. Ozone production decreased with decreased flow rate, the same effect observed in typical ozone generator mapping curves (Stover, 1982). The next six experiments ran under similar power and flow rates, but with less humidity in the air stream. This translates to a relative humidity of 21% or the humidity inherent in the compressed air cylinder. These experiments showed the same trend of increased

production with increased flow rate. However, the production rate was higher than in the experiments with higher humidity. The final three experiments ran at a higher supplied power of 100 watts, with 21% humidity, and at variable flow rates. The results showed an even greater ozone production rate. Figure 15 graphically illustrates the ozone production rate under various conditions of flow rate, humidity, and power.

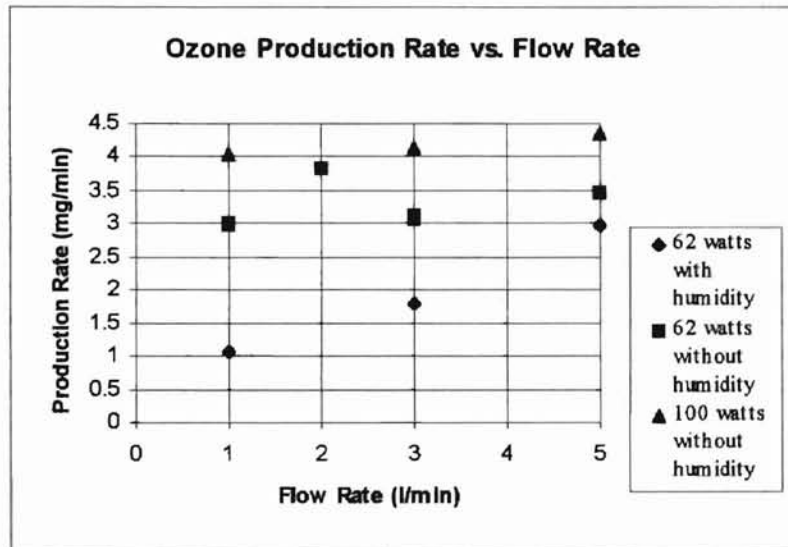


Figure 15: Ozone Production Rate versus Air Flow Rate

The general trend of Figure 15 dictates an increase in production when only flow rate changes. More ozone production results from an increase in power as well as a decrease in air stream relative humidity. In general, some amount of ozone production results if oxygen is present in the plasma air stream. However, a filter system containing rusted steel wool is a sufficient ozone scrubbing unit and will remove any harmful concentrations of ozone (Melnick, 1996).

## Single Pass Results

Single pass ethylene destruction tests satisfied the fourth experimental objective. The setup and experimental method followed the criteria discussed earlier. Table 6 gives the conditions and results of the eleven separate single pass runs.

Run	Flow Rate	Primary Power	Ethylene Destruction	Average	Standard Deviation
	(l/min)	(Watts)	(%)	(%)	(x 1.5)
1	1	54	72.2		
2	3	54	66.2	69.4	4.5
3	5	54	69.7		
4	1	80	78.2		
5	3	80	72.2	75.9	4.8
6	5	80	77.2		
7	1	115	61.1		
8	3	115	78.1	68.1	13.3
9	5	115	65.3		
10	1	40	40.5	43.6	
11	5	40	46.7		

Table 6: Conditions and Results of Single Pass Destruction Runs

The single pass runs ran under different conditions of power and flow rate. Power varied from 40, 54, 80, and 115 watts; flow rate varied from 1, 3, and 5 liters/minute.

Thermistors monitored influent and effluent gas streams to assure temperatures less than 50°F, which also assured a relative humidity greater than 90% (Appendix E). The combined samples resulted in an average ethylene destruction for each run. Appendix E contains the original data used to calculate the average destruction percentages.

Figure 16 shows the percent destruction versus power supplied to the transformer.

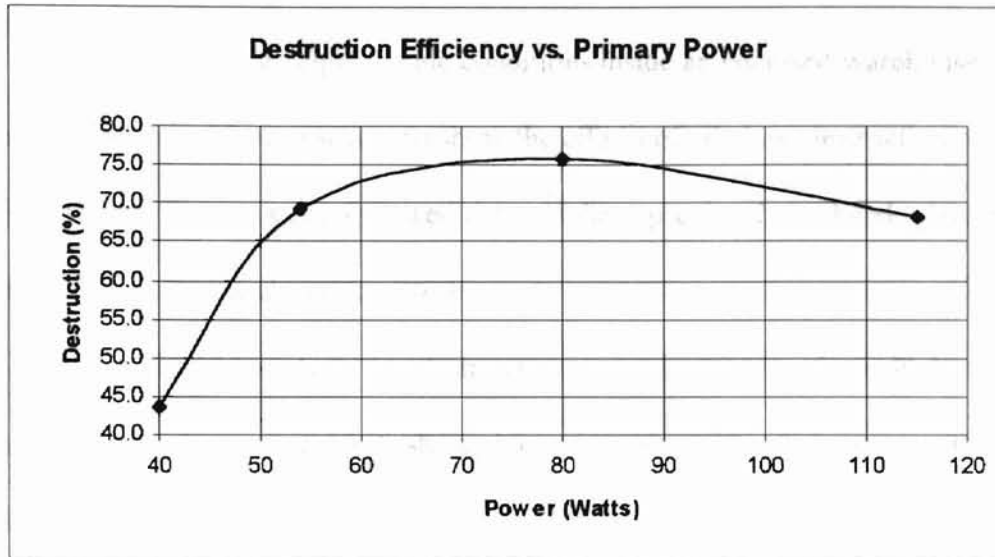


Figure 16: Destruction Efficiency versus Supplied Primary Power

The destruction percentages equal the average from 1, 3, and 5 l/min runs from each power setting. For the lowest power setting, destruction percentage equals the averages from the 1 and 5 l/min runs. As illustrated in Figure 16, the destruction efficiency appears to level off and decrease when the transformer receives more than 80 watts of power. However, a review of standard deviations from the average indicates a drift in the precision of these data points and the actual percent destruction is probably only leveling off. This leveling off effect may be due to a kinetic equilibrium effect inside the reactor where at high enough powers the destroyed ethylene has enough energy to reform.

## Closed Loop Results

Closed loop testing helped mimic conditions inside an enclosed warehouse. The objective of the closed loop test was to show the effects of ethylene destruction through a recycling system. System setup followed the guidelines previously outlined. Appendix F contains raw data for the closed loop tests.

The first closed loop test, the plastic vat test, used a 23-liter plastic high residence vat. As Figure 17 shows, the results showed a reasonably stable ethylene concentration persisting after the first 24-minute cycle.

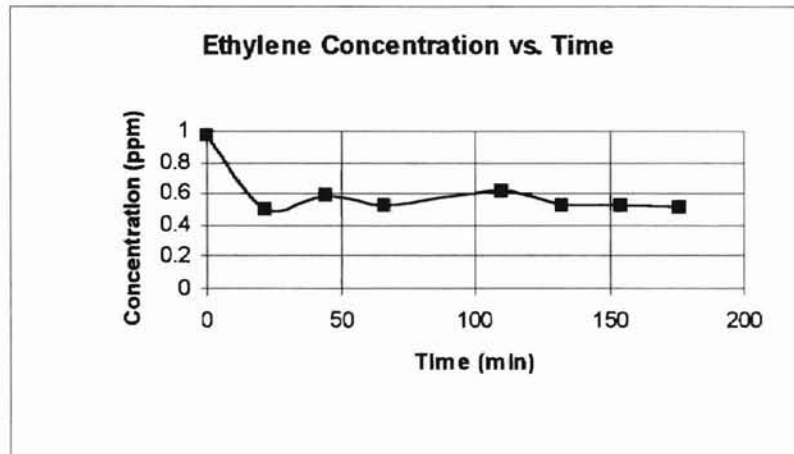


Figure 17: Closed Loop, Plastic Vat Test Results

Several explanations exist for the possible reasons behind this effect. At the time of the test, the reason hypothesized was adsorption onto the inner lining of the plastic vat. Therefore, the next closed loop test used a metal high residence vat to determine the feasibility of plastic adsorption. This modification occurred to avoid ethylene adsorption.



As Figure 18 illustrates, the same basic phenomena occurred with a stable ethylene concentration appearing after the third cycle (72 minutes).

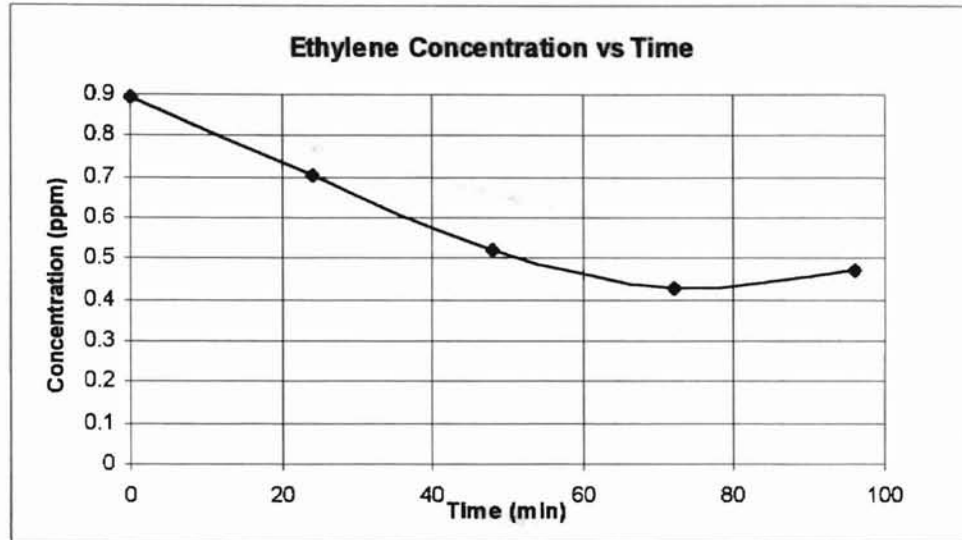


Figure 18: Closed Loop, Metal Vat Test Results

The results of test number two were also similar to test number one in that the concentration of ethylene dropped approximately 0.5 ppm (50% destruction). The next test, test number three, determined the effects of ethylene destruction after a duration of 17 cycles or 6 hours and 48 minutes. The hypothesis was that a long run time would result in a gradual drop in ethylene concentration. Table 7 gives the result of the long-term experiment.

Cycle	Time (min)	Ethylene Concentration ppm
0	0	0.91
17	408	0.42

Table 7: Closed Loop, Seventeen Cycle Test Results

As shown in Table 7, the resulting ethylene concentration was still indicative of a drop of approximately 0.5 ppm (50% destruction). Therefore, test number four ran at a lower

initial ethylene concentration to determine the resulting effects on destruction. Figure 19 illustrates results of test number 4.

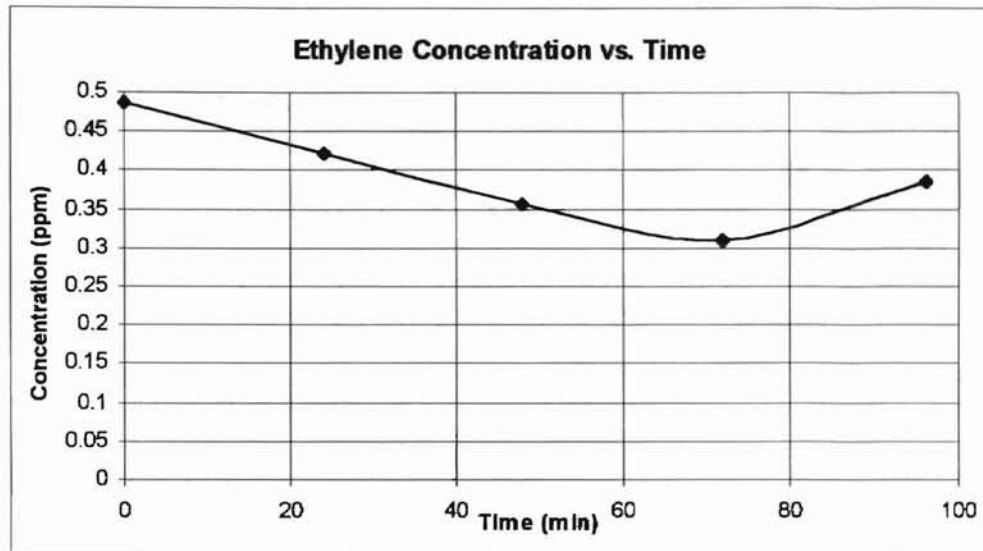


Figure 19: Closed Loop, Low Concentration Test Results

Test number four showed a decreased overall difference (40% destruction) in ethylene concentration. However, after the third cycle (72 minutes) ethylene concentration again appears to have reached an equilibrium stage. For the fifth test, the air injection test, a Teflon syringe introduced 10 ml of air into the closed loop system after 121 minutes or the end of the fifth cycle. This test ran based on the known ozone production of the plasma reactor. An injection of air would allow the reactor to form more ozone. If ozone was the only effective ethylene destruction process, then an air injection would have some effect on ethylene concentration.

Figure 20 illustrates the results of test number 5.

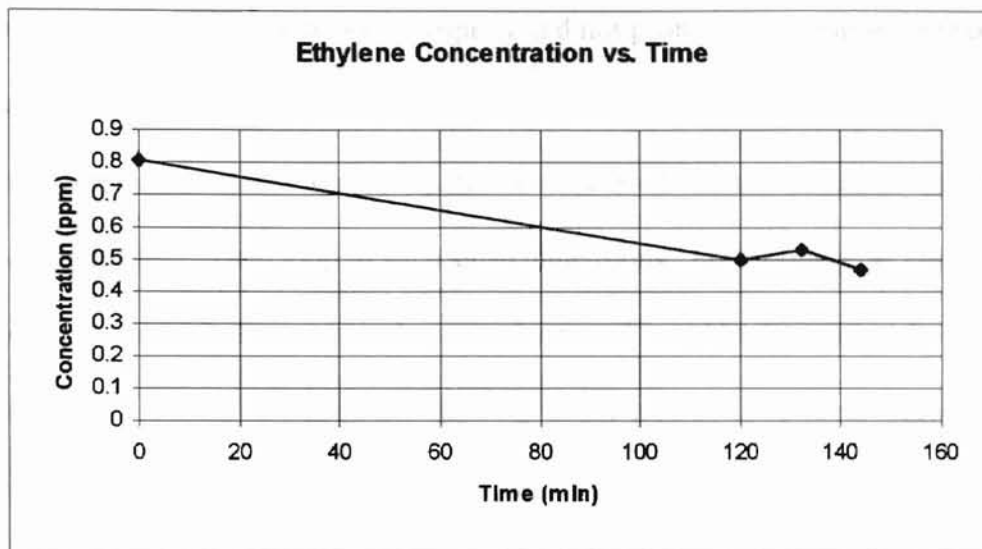


Figure 20: Closed Loop, Air Injection Test Results

Figure 20 shows that an air injection showed no effect on ethylene concentration (45% destruction). Therefore, for test number 6, the oxygen injection test, a Teflon syringe introduced 10 ml of pure oxygen at 121 minutes and 145 minutes or after cycles 5 and 6, respectively. Figure 21 illustrates the results of closed loop test 6.

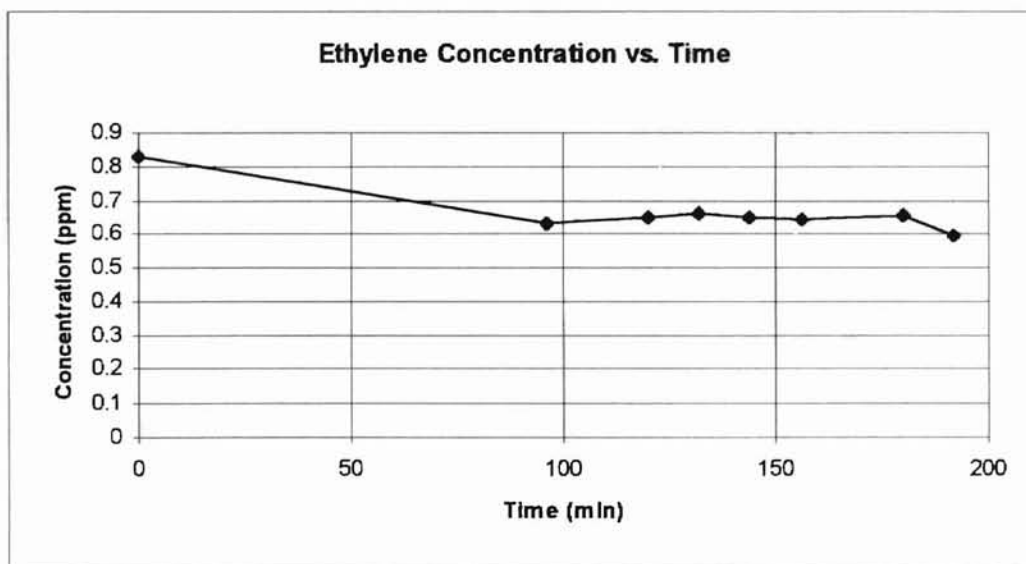


Figure 21: Closed Loop, Oxygen Injection Test Results

Based on the results of the six closed loop tests (<50% destruction), the conclusion was that the recycle system was operating properly and not prone to ethylene adsorption on its interior or dependent upon ozone formation in the reactor to destroy ethylene. Therefore, the hypothesis was the concentration equilibrium occurred because of kinetic equilibrium which exists inside a closed loop of such small dimensions. For example, as ethylene initially passed through the reactor, electrons destroyed it and broke it into a by-product. However, as the recycle continued and the by-product entered the plasma reactor, it would in turn be destroyed and transformed back into ethylene. Another possible hypothesis is the creation of a "light" by-product which escapes the analysis equipment concurrently with ethylene. The effect of such a by-product would be to give a falsely high analysis of ethylene concentration.

## **By-Product Analysis Results**

The closed loop system helped to determine by-products formed by the plasma reaction with ethylene. The system ran a completion of five cycles. At the end of the fifth cycle a summa canister evacuated the contents of the high residence vat. The summa canister contents underwent analysis following the previously discussed procedure. Table 8 gives the findings of the by-product analysis.

<b>Compound</b>	<b>Concentration (ppbv)</b>
Acetone	353.09
4-Methyl-2-Pentanone	42.17
1,2-Dichloroethane	10.12
Toluene-d8	10.18
4-Bromofluorobenzene	10.10
(Propene)*	13.98
(Hexane, 2-methyl-)	22.03
Unknown 3 (no match)	29.05
(Heptane, 2-methyl-)	14.37
(Hexane, 2,4-dimethyl-)	18.88
Phenol	36.37
(Cyclohexane, 1,3,5-trimethyl-)	25.04
Benzothiazole	29.94

\* ( ) indicates a probable match

Table 8: Reactor By-Product Identification

It should be noted that ethylene and other smaller molecular weight compound were not analyzed for with this by-product test. The two compounds of significant concentration are acetone and 4-methyl-2-pentanone. However, both of these components are in the parts-per-billion range and therefore do not pose a significant threat. The acetone is already a product in the compressed ethylene tank (Powers, 1996). The ethylene bottling process utilizes an ethylene/acetone mixture due to the explosive properties of ethylene. Also, in accordance with objective number five, none of the by-products identified seemed to be in harmful concentrations or of a harmful nature.

## Costs

Cost of air per day for 29

Table 9 outlines the basic system capital cost for the equipment necessary to create the plasma system used for this research.

Item	Reference / Item Number	Cost (\$)
Liebig Condenser Tube	Kimble/Kontes Glass Catalog, KK-148 - Item # 447000-2420	64.25
Gaseous Tube Transformer	Glantz and Sons, Tulsa, OK - Item # 15060 P	121.48
High Voltage Probe	Hewlett Packard, Test and Measurement Catalog, 1996 - Item # HP 1137A	209.00
Variac	Hewlett Packard, Test and Measurement Catalog, 1996 - Item # HP E3612A	300.00
Frequency Generator	Hewlett Packard, Test and Measurement Catalog, 1996 - Item # HP 3325B	7835.00
Multimeter	Hewlett Packard, Test and Measurement Catalog, 1996 - Item # HP 973A	290.00

Table 9: Plasma System Capital Costs

Use of the variac in place of the frequency generator greatly reduces system capital costs. A variac is basically a variable transformer which cost \$300, making the cost of the system about \$984.73. On the other hand, a frequency generator is a complicated piece of equipment which typically markets around \$7,835, making the system cost \$8519.73. For a true commercial system several simplifications such as a fixed-voltage power supply, fixed-frequency generator, and built-in multimeter and high voltage probe further reduce the price. However, at either price, the system would prove beneficial in the money saved from undamaged produce.

Run costs can be estimated from the amount of power supplied to the plasma unit. At the maximum power of 115 watts, the cost to run the unit would be \$0.012 per hour. This number is based on OG&E electricity rates of \$0.1061 per kilowatt-hour. This run cost converts to \$0.29 per day. Therefore, assuming a 24 hour run time and constant

concentration of ethylene, a plasma unit this size could treat 153 ft<sup>3</sup> of air per day for 29 cents.

## Conclusions / Recommendations

The liquid electrode plasma system seemed to meet all of the requirements of the stated objectives.

- modification to run at optimum frequency of 60 hertz
- negligible effects on effluent temperatures averaging an increase of 1.87 °F/day
- ozone production rates monitored under varying conditions of flow rate, humidity, and supplied power, with a maximum production rate of 4.35 mg/min
- single pass ethylene destruction tests monitored to determine a maximum destruction efficiency of 78.2%
- closed loop ethylene destruction tests monitored to determine minimal amounts of any ethylene destruction created by-products
- capital and operating costs assessed resulting in minimum system component cost of \$984.73 and system operating cost of \$0.012 per hour

Considering the results of the research, a liquid electrode plasma system seems to have potential be an effective and efficient alternative to other previously discussed ethylene control and removal technologies.



All of the research discussed above established a groundwork for the use of plasma technology in the fresh fruit and vegetable industry. Recommendations for further research include the following:

- research into transformer optimization to achieve higher power outputs
- research into better controlled temperature experiments to remove environmental temperature affecting variables such as heating units
- research into ozone production control as it emits from a plasma system
- research into the effects of higher ethylene concentrations on destruction efficiency
- further quantification and qualification of ethylene destruction by-products to determine the effects of acetone native to compressed ethylene cylinders
- research into prolonged run times to determine an average long-term maintenance cost

The preceding recommendations contain possible areas of further research. Based on the apparent success of plasma systems in the destruction of ethylene, their future seems to be “shining bright” in the food storage field.

## References

- Anderson, J. Personal communication with researcher. Oklahoma State University, 20 October 1996.
- APHA, AWWA, and WPCF. "Iodometric Determination of Ozone," Standard Methods: for the Examination of Water and Wastewater. 15<sup>th</sup> edition, 1980.
- Ashby B. H. et al. Protecting Perishable Foods: During Transport by Truck. USDA Agricultural Handbook 669, 1987.
- El-Blidi et al. "Ethylene removal for long term conservation of fruits and vegetables." Food Quality and Preference 4 (3), 1993, pg 199-126.
- Encarta, "Plasma (physics)," Microsoft ®. Copyright © 1994 Microsoft Corporation. Copyright © 1994 Funk & Wagnalls Corporation.
- Glantz and Sons. Personal communication with Dr. John Veenstra (price quote). 20 December 1995.
- Glockler, G. and S. C. Lind. The Electro-Chemistry of Gases and Other Dielectrics. John Wiley and Sons, NY City, NY, 1938.
- Hewlett Packard, Test and Measurement Catalog, 1996.
- Hurst, M. C. Destruction of Carbon Tetrachloride in an Alternating Current Plasma Reactor. Thesis, Oklahoma State University, Stillwater, 1993.
- Kader, A. A. et al. Postharvest Technology of Horticultural Crops. Berkeley, University of California, 1985.
- Kimble/Kontes Glass Catalog, KK-148, 1996.
- Marcellin, P. "Nouvelles tendances de la conservation des fruits et légumes par réfrigération." RGF, 3, 1982, pg 143-151.
- Melnick, R. "Put a charge in your storage system. Advance in storage technology uses electrically charged corona to destroy molds, convert ethylene." Fruit Grower. January, 1996.
- Miller, A. Meteorology. Charles E. Merrill Publishing Co., Columbus, Ohio, 1971.
- OG & E. Personal communication with Mark Isom (rate quote). 19 March 1996.

Parker, G. W. Conceptual Design of an Industrial Applicable Plasma Reactor. Thesis, Oklahoma State University, Stillwater, 1994.

Pech, J. C. and Latch, A. "Applications récentes du contrôle de la synthèses et des effets de l'éthylène en physiologie après récolte." 4ème Colloque sur la Recherche Fuitière. Eds. P. Crossa-Raynuad & J. Ulrich, Bordeaux, 1985, pg 149-162.

Pech, J. C. et al. "Contrôle de la synthèse et des effets de l'éthylène. 2ème Colloque sur les substances de croissance et leur utilisation en agriculture." ANPP, Paris, Vol. I, 1987, pg 111-122.

Powers, R. 1996. Personal communication with GC/MS operator. Stover and Associates, 23 November 1996.

Stover, E. L. "Optimizing Operational Control of Ozone Disinfection." Paper presented at the Second National Symposium on Municipal Wastewater Disinfection. Orlando, Florida, 1982.

USEPA. "Compendium Method TO-14", document number EPA-600/4-84-041, 1988.

USEPA. "Compendium of Methods for the Determination of Toxic Organic Compounds in Ambient Air," document number EPA-600/4-84-041, 1988.

Yoo, H. Performance and Economics of Air Stripping Tower with Off-Gas Control by either Gas-Phase Carbon Adsorption or Plasma Reactor in Comparison to Liquid-Phase Carbon Adsorption. PhD Dissertation, Oklahoma State University, Stillwater, 1991.



PSYCHOMETRIC TABLES

Temperature (°F)	Probe 1 (ohms)	Probe 2 (ohms)	Probe 3 (ohms)	Probe 4 (ohms)
32	19.80	19.70		
33	19.90	19.70	19.65	19.72
34			19.15	19.09
35			17.91	18.35
36			17.87	17.89
37	17.50		16.93	17.70
38	16.90	17.11	16.87	17.33
39			16.18	16.70
40			15.82	16.26
42			15.54	15.02
43	14.75	14.52		
48	12.72	12.75		
62			7.39	7.14
66	7.95	7.96		
70			6.34	6.24

Thermistor Calibration Data

**PSYCHOMETRIC TABLES**  
(Miller, 1971)

Table A Dew-Point Temperature (°F) and Saturation Vapor Pressure (in. Hg) (Pressure = 30 in. Hg)

Air temperature (°F)	Vapor pressure (in. Hg)	Depression of wet-bulb thermometer (°F)														
		1	2	3	4	5	6	7	8	9	10	15	20	25	30	35
20	0.110	16	12	8	2	-7	-21									
25	0.135	22	19	15	10	5	-3	-15	-51							
30	0.166	27	25	21	18	14	8	2	-7	-25						
35	0.203	33	30	28	25	21	17	13	7	0	-11					
40	0.248	38	35	33	30	28	25	21	18	13	7					
45	0.300	43	41	38	36	34	31	28	25	22	18					
50	0.362	48	46	44	42	40	37	34	32	29	26	0				
55	0.436	53	51	50	48	45	43	41	38	36	33	15				
60	0.522	58	57	55	53	51	49	47	45	43	40	25	-8			
65	0.622	63	62	60	59	57	55	53	51	49	47	34	14			
70	0.739	69	67	65	64	62	61	59	57	55	53	42	26	-11		
75	0.875	74	72	71	69	68	66	64	63	61	59	49	36	15		
80	1.032	79	77	76	74	73	72	70	68	67	65	56	44	28	-7	
85	1.214	84	82	81	80	78	77	75	74	72	71	62	52	39	19	
90	1.422	89	87	86	85	83	82	81	79	78	76	69	59	48	32	1
95	1.661	94	93	91	90	89	87	86	85	83	82	74	66	56	43	24
100	1.933	99	98	96	95	94	93	91	90	89	87	80	72	63	52	37
105	2.244	104	103	101	100	99	98	96	95	94	93	86	78	70	61	48
110	2.597	109	108	106	105	104	103	102	100	99	98	91	84	77	68	57
115	2.996	114	113	112	110	109	108	107	106	104	103	97	90	83	75	65

Table B Relative Humidity (per cent) (Pressure = 30 in. Hg)

Air temperature (°F)	Depression of wet-bulb thermometer (°F)														
	1	2	3	4	5	6	7	8	9	10	15	20	25	30	35
20	85	70	55	40	26	12									
25	87	74	62	49	37	25	13	1							
30	89	78	67	56	46	36	26	16	6						
35	91	81	72	63	54	45	36	29	19	10					
40	92	83	75	68	60	52	45	37	29	22					
45	93	86	78	71	64	57	51	44	38	31					
50	93	87	80	74	67	61	55	49	43	38	10				
55	94	88	82	76	70	65	59	54	49	43	49				
60	94	89	84	78	73	68	63	58	53	48	26	5			
65	95	90	85	80	75	70	66	61	56	52	31	12			
70	95	90	86	81	77	72	68	64	59	55	36	19	3		
75	96	91	86	82	78	74	70	66	62	58	40	24	9		
80	96	91	87	83	79	75	72	68	64	61	44	29	15	3	
85	96	92	88	84	80	76	73	69	66	62	46	32	20	8	
90	96	92	89	85	81	78	74	71	68	65	49	36	24	13	3
95	96	93	89	85	82	79	75	72	69	66	51	38	27	17	7
100	96	93	89	86	83	80	77	73	70	68	54	41	30	21	12
105	97	93	90	87	83	80	77	74	71	69	55	43	33	23	15
110	97	93	90	87	84	81	78	75	73	70	57	46	36	26	18
115	97	94	91	88	85	82	79	76	74	71	58	47	37	28	21

**Appendix B:**

**Transformer**

**Optimization**

**Data**

Voltage (volts)	30	40	50	60	70	80	90	100	110	120
Frequency (hertz)	Current (mA)									
50						578	687	828	1006	1231
60						461	526	602	704	825
70						393	440	493	554	629
80						342	390	430	474	524
90						303	353	388	420	463
100					248	302	338	368	398	427
110					225	288	323	350	376	400
120					206	274	308	336	362	386
130					190	267	306	337	367	397
140					176	275	316	358	395	433
150					165	296	351	406	452	490
160					155	333	384	422	450	475
170					146	333	370	404	436	466
180					138	315	356	398	435	475
190					133	303	355	397	442	488
200				117	213	294	354	407	459	511
210				111	183	292	362	422	486	546
220				109	121	299	377	446	520	588
230				106	118	310	396	474	559	644
240				104	118	323	415	512	606	707
250				105	118	343	454	560	674	
260				104	119	377	496	617	744	
280				109	127	446	606	774		
300				120	350	550	782			
320				129	444	720	1041			
340				141	578	983				
360			132	162	799					
380			150	512	1062					
400			171	694	1200					
420			196	818	1215					
440			223	859	1159					
460		201	579	869	1087					
480		232	617	831	1031	1199	1366			
500	192	430	628	798	974	1120	1258	1388		
520	226	482	628	772	913	1044	1168	1291	1410	1522
540	308	509	623	747	862	980	1095	1203	1309	1418
560	394	519	618	722	824	927	1039	1131	1234	1330
580	425	526	611	702	787	882	970	1070	1162	1252
600	439	528	603	676		843		1012		1181
650	454		586			769		903		1045
700	437		564			723		834		951

Transformer Primary Current Data



Voltage (volts)	30	40	50	60	70	80	90	100	110	120
Frequency (hertz)	Power (watts)									
50						46.24	61.83	82.8	110.66	147.72
60						36.88	47.34	60.2	77.44	99
70						31.44	39.6	49.3	60.94	75.48
80						27.36	35.1	43	52.14	62.88
90						24.24	31.77	38.8	46.2	55.56
100					17.36	24.16	30.42	36.8	43.78	51.24
110					15.75	23.04	29.07	35	41.36	48
120					14.42	21.92	27.72	33.6	39.82	46.32
130					13.3	21.36	27.54	33.7	40.37	47.64
140					12.32	22	28.44	35.8	43.45	51.96
150					11.55	23.68	31.59	40.6	49.72	58.8
160					10.85	26.64	34.56	42.2	49.5	57
170					10.22	26.64	33.3	40.4	47.96	55.92
180					9.66	25.2	32.04	39.8	47.85	57
190					9.31	24.24	31.95	39.7	48.62	58.56
200				7.02	14.91	23.52	31.86	40.7	50.49	61.32
210				6.66	12.81	23.36	32.58	42.2	53.46	65.52
220				6.54	8.47	23.92	33.93	44.6	57.2	70.56
230				6.36	8.26	24.8	35.64	47.4	61.49	77.28
240				6.24	8.26	25.84	37.35	51.2	66.66	84.84
250				6.3	8.26	27.44	40.86	56	74.14	
260				6.24	8.33	30.16	44.64	61.7	81.84	
280				6.54	8.89	35.68	54.54	77.4		
300				7.2	24.5	44	70.38			
320				7.74	31.08	57.6	93.69			
340				8.46	40.46	78.64				
360			6.6	9.72	55.93					
380			7.5	30.72	74.34					
400			8.55	41.64	84					
420			9.8	49.08	85.05					
440			11.15	51.54	81.13					
460		8.04	28.95	52.14	76.09					
480		9.28	30.85	49.86	72.17	95.92	122.94			
500	5.76	17.2	31.4	47.88	68.18	89.6	113.22	138.8		
520	6.78	19.28	31.4	46.32	63.91	83.52	105.12	129.1	155.1	182.64
540	9.24	20.36	31.15	44.82	60.34	78.4	98.55	120.3	143.99	170.16
560	11.82	20.76	30.9	43.32	57.68	74.16	93.51	113.1	135.74	159.6
580	12.75	21.04	30.55	42.12	55.09	70.56	87.3	107	127.82	150.24
600	13.17	21.12	30.15	40.56		67.44		101.2		141.72
650	13.62		29.3			61.52		90.3		125.4
700	13.11		28.2			57.84		83.4		114.12

Transformer Power Data

Date: \_\_\_\_\_  
Page No: \_\_\_\_\_  
Page No: \_\_\_\_\_

## **Appendix C:**

### **Temperature**

#### **Test Data**

Elapsed Time	Effluent / Probe 3	Probe 3 Temperature	Influent / Probe 1	Probe 1 Temperature	Inner Electrode Temperature	Outer Electrode Temperature
(min)	(ohms)	(°F)	(ohms)	(°F)	(°F)	(°F)
0	5.76	69.02	6.95	66.80	66	72
7	5.74	69.08	6.94	66.85	70	72
12	5.74	69.08	6.93	66.88	71	72
17	5.72	69.14	6.88	67.01	72	72
22	5.72	69.14	6.88	67.01	73	73
27	5.72	69.14	6.87	67.04	74	73
32	5.71	69.17	6.86	67.06	75	73
62	5.67	69.28	6.79	67.25	80	73
182	5.57	69.57	6.62	67.73	81	74
229	5.59	69.51	6.60	67.78	81	74
345	5.49	69.77	6.53	67.99	82	75
435	5.49	69.77	6.50	68.07	82	75
486	5.43	69.94	6.46	68.18	84	76
579	5.52	69.71	6.48	68.13	85	77
700	5.46	69.85	6.49	68.10	85	77

Temperature Test Data

Run	Flow (l/min)	in (cm)	Relative Humidity (%)	Primary Power (watts)	Titration (mL)
4				62	12.8
5				62	12.8
6				62	12.8
7				62	12.8
8				62	12.8

### Appendix D: ---

### Ozone Gas Analysis

### Titration Data

Run	Flow Rate	Run Time	Relative Humidity	Primary Power	Titrant
	(l/min)	(min)	(%)	(watts)	(ml)
1	5	5.0	60	62	12.5
2	3	5.0	60	62	7.5
3	1	9.0	60	62	7.9
4	1	8.0	21	62	20.1
5	2	3.0	21	62	9.6
6	3	2.0	21	62	5.2
7	5	2.0	21	62	5.8
8	3	2.0	21	62	5.1
9	1	5.0	21	62	12.4
10	5	2.5	21	100	9.1
11	3	4.0	21	100	13.8
12	1	4.5	21	100	15.2

Ozone Production Titration Test Data

Table

**Appendix E:**

**Single Pass**

**Run Data**

**Run 1**

Time (min)	Probe 1 (ohms)	Temperature (°F)
0	16.04	41.32
7	15.91	41.69
12	16.19	40.89
18	15.97	41.52
22	16.20	40.86
27	16.10	41.15

Influent Temperatures

Time (min)	Probe 3 (ohms)	Temperature (°F)
0	14.25	45.61
7	14.43	45.12
12	15.03	43.46
18	15.13	43.18
22	15.11	43.22
27	15.08	43.31

Effluent Temperatures

Time (min)	Probe 2 / dry (ohms)	Temperature (°F)	Probe 2 / wet (ohms)	Temperature (°F)	Relative Humidity (%)
0	15.62	42.4	15.80	41.9	>90
25	16.12	41.0	16.43	40.1	>90

Influent Humidity

Time (min)	Probe 4 / dry (ohms)	Temperature (°F)	Probe 4 / wet (ohms)	Temperature (°F)	Relative Humidity (%)
0	14.36	45.6	14.63	44.9	>90
25	15.23	43.3	15.35	43.0	>90

Effluent Humidity

Inf / Eff	Needle	Time (min)	Ethylene (peak area)	Ethylene (ppm)
Influent	1	0	2447	0.97
Effluent	2	5	722	0.29
Effluent	3	10	636	0.25
Effluent	4	15	739	0.29
Influent	5	15	2531	1.00
Effluent	6	20	5088	2.02*
Influent	7	25	2573	1.02
Effluent	8	30	3039	1.21*

\* Results deleted due to testing problems.

Averages		
Influent (ppm)	Effluent (ppm)	% Destruction
1.00	0.28	72.2

Ethylene Destruction

## Run 2

Time (min)	Probe 1 (ohms)	Temperature (°F)
0	16.74	39.35
7	17.27	37.86
12	17.36	37.60
18	17.27	37.86
22	17.37	37.57
27	17.30	37.77

Influent Temperatures

Time (min)	Probe 3 (ohms)	Temperature (°F)
0	14.85	43.95
7	14.39	45.22
12	14.21	45.72
18	13.97	46.37
22	14.12	45.96
27	13.89	46.58

Effluent Temperatures

Time (min)	Probe 2 / dry (ohms)	Temperature (°F)	Probe 2 / wet (ohms)	Temperature (°F)	Relative Humidity (%)
0	16.65	39.5	16.79	39.1	>90
25	16.86	38.9	17.18	38.0	>90

Influent Humidity

Time (min)	Probe 4 / dry (ohms)	Temperature (°F)	Probe 4 / wet (ohms)	Temperature (°F)	Relative Humidity (%)
0	15.01	43.9	15.16	43.5	>90
25	14.29	45.8	14.41	45.5	>90

Effluent Humidity

Inf / Eff	Needle	Time (min)	Ethylene (peak area)	Ethylene (ppm)
Influent	1	0	2507	0.99
Effluent	2	5	858	0.34
Effluent	3	10	714	0.28
Effluent	4	15	1049	0.42
Influent	5	15	6607	2.62*
Effluent	6	20	5515	2.19*
Influent	7	25	3383	1.34*
Effluent	8	30	2655	1.05

\* Results deleted due to testing problems.

Averages		
Influent (ppm)	Effluent (ppm)	% Destruction
1.02	0.35	66.2

Ethylene Destruction



### Run 3

Time (min)	Probe 1 (ohms)	Temperature (°F)
0	16.81	39.15
7	16.70	39.46
12	16.50	40.03
18	16.44	40.20
22	16.66	39.57
27	16.00	41.43

Influent Temperatures

Time (min)	Probe 3 (ohms)	Temperature (°F)
0	13.69	47.14
7	12.71	49.86
12	12.68	49.95
18	12.67	49.97
22	12.73	49.80
27	12.73	49.80

Effluent Temperatures

Time (min)	Probe 2 / dry (ohms)	Temperature (°F)	Probe 2 / wet (ohms)	Temperature (°F)	Relative Humidity (%)
0	16.65	39.5	16.68	39.4	>90
25	15.83	41.8	16.12	41.0	>90

Influent Humidity

Time (min)	Probe 4 / dry (ohms)	Temperature (°F)	Probe 4 / wet (ohms)	Temperature (°F)	Relative Humidity (%)
0	13.84	47.0	13.92	46.8	>90
25	12.79	49.8	13.09	49.0	>90

Effluent Humidity

Inf / Eff	Needle	Time (min)	Ethylene (peak area)	Ethylene (ppm)
Influent	1	0	2312	0.92
Effluent	2	5	727	0.29
Effluent	3	10	729	0.29
Effluent	4	15	590	0.23
Influent	5	15	4776	1.90*
Effluent	6	20	833	0.33
Influent	7	25	1190	0.47*
Effluent	8	30	2433	0.97

\* Results deleted due to testing problems.

Averages		
Influent (ppm)	Effluent (ppm)	% Destruction
0.94	0.29	69.7

Ethylene Destruction

### Run 4

Time (min)	Probe 1 (ohms)	Temperature (°F)
0	15.16	43.77
7	14.97	44.32
12	15.25	43.54
18	15.45	42.97
22	15.52	42.77
27	15.45	42.97

Influent Temperatures

Time (min)	Probe 3 (ohms)	Temperature (°F)
0	13.59	47.42
7	13.87	46.65
12	13.88	46.63
18	13.95	46.43
22	13.89	46.58
27	13.80	46.84

Effluent Temperatures

Time (min)	Probe 2 / dry (ohms)	Temperature (°F)	Probe 2 / wet (ohms)	Temperature (°F)	Relative Humidity (%)
0	15.16	43.7	15.37	43.1	>90
25	15.41	43.0	15.48	42.8	>90

Influent Humidity

Time (min)	Probe 4 / dry (ohms)	Temperature (°F)	Probe 4 / wet (ohms)	Temperature (°F)	Relative Humidity (%)
0	13.65	47.5	13.77	47.2	>90
25	14.48	45.3	14.52	45.2	>90

Effluent Humidity

Inf / Eff	Needle	Time (min)	Ethylene (peak area)	Ethylene (ppm)
Influent	1	0	168	0.07*
Effluent	2	5	544	0.22
Effluent	3	10	564	0.22
Effluent	4	15	329	0.13
Influent	5	15	2323	0.92
Effluent	6	20	518	0.21
Influent	7	25	2327	0.92
Influent	8	30	2082	0.83

\* Results deleted due to testing problems.

Averages		
Influent (ppm)	Effluent (ppm)	% Destruction
0.89	0.19	78.2

Ethylene Destruction

### Run 5

Time (min)	Probe 1 (ohms)	Temperature (°F)
0	16.89	38.95
7	16.87	39.00
12	16.74	39.35
18	16.72	39.40
22	16.93	38.83
27	16.72	39.40

Influent Temperatures

Time (min)	Probe 3 (ohms)	Temperature (°F)
0	14.39	45.20
7	13.95	46.43
12	13.71	47.08
18	13.67	47.21
22	13.66	47.23
27	13.56	47.51

Effluent Temperatures

Time (min)	Probe 2 / dry (ohms)	Temperature (°F)	Probe 2 / wet (ohms)	Temperature (°F)	Relative Humidity (%)
0	16.89	38.8	17.04	38.4	>90
25	16.61	39.6	16.65	39.5	>90

Influent Humidity

Time (min)	Probe 4 / dry (ohms)	Temperature (°F)	Probe 4 / wet (ohms)	Temperature (°F)	Relative Humidity (%)
0	14.48	45.3	14.63	44.9	>90
25	13.73	47.3	13.92	46.8	>90

Effluent Humidity

Inf / Eff	Needle	Time (min)	Ethylene (peak area)	Ethylene (ppm)
Influent	1	0	2292	0.91
Effluent	2	5	613	0.24
Effluent	3	10	633	0.25
Effluent	4	15	581	0.23
Influent	5	15	2224	0.88
Effluent	6	20	641	0.25
Influent	7	25	2286	0.91
Influent	8	30	2082	0.83

Averages		
Influent (ppm)	Effluent (ppm)	% Destruction
0.88	0.24	72.2

Ethylene Destruction

### Run 6

Time (min)	Probe 1 (ohms)	Temperature (°F)
0	15.57	42.63
7	15.26	43.52
12	15.11	43.92
18	15.14	43.83
22	15.08	44.00
27	14.94	44.40

Influent Temperatures

Time (min)	Probe 3 (ohms)	Temperature (°F)
0	13.87	46.65
7	12.82	49.56
12	13.05	48.90
18	12.66	50.00
22	12.73	49.80
27	12.69	49.90

Effluent Temperatures

Time (min)	Probe 2 / dry (ohms)	Temperature (°F)	Probe 2 / wet (ohms)	Temperature (°F)	Relative Humidity (%)
0	15.41	43.0	15.48	42.8	>90
25	14.88	44.5	14.95	44.3	>90

Influent Humidity

Time (min)	Probe 4 / dry (ohms)	Temperature (°F)	Probe 4 / wet (ohms)	Temperature (°F)	Relative Humidity (%)
0	13.84	47.0	13.92	46.8	>90
25	13.17	48.8	13.50	47.9	>90

Effluent Humidity

Inf / Eff	Needle	Time (min)	Ethylene (peak area)	Ethylene (ppm)
Influent	1	0	2292	0.91
Effluent	2	5	548	0.22
Effluent	3	10	522	0.21
Effluent	4	15	446	0.18
Influent	5	15	2238	0.89
Effluent	6	20	557	0.22
Influent	7	25	2298	0.91
Influent	8	30	2262	0.90

Averages		
Influent (ppm)	Effluent (ppm)	% Destruction
0.90	0.21	77.2

Ethylene Destruction

### Run 7

Time (min)	Probe 1 (ohms)	Temperature (°F)
0	14.93	44.43
7	14.50	45.63
12	14.54	45.52
18	14.37	46.00
22	14.30	46.20
27	14.37	46.00

Influent Temperatures

Time (min)	Probe 3 (ohms)	Temperature (°F)
0	14.13	45.94
7	14.41	45.16
12	14.48	44.97
18	14.34	45.35
22	14.16	45.85
27	14.24	45.63

Effluent Temperatures

Time (min)	Probe 2 / dry (ohms)	Temperature (°F)	Probe 2 / wet (ohms)	Temperature (°F)	Relative Humidity (%)
0	14.91	44.4	15.05	44.0	>90
25	14.70	45.0	15.05	44.0	>90

Influent Humidity

Time (min)	Probe 4 / dry (ohms)	Temperature (°F)	Probe 4 / wet (ohms)	Temperature (°F)	Relative Humidity (%)
0	14.36	45.6	14.63	44.9	>90
25	15.23	43.3	15.35	43.0	>90

Effluent Humidity

Inf / Eff	Needle	Time (min)	Ethylene (peak area)	Ethylene (ppm)
Influent	1	0	2310	0.92
Effluent	2	5	953	0.38
Effluent	3	10	1042	0.41
Effluent	4	15	693	0.28
Influent	5	15	2054	0.82
Effluent	6	20	773	0.31
Influent	7	25	1672	0.66*
Influent	8	30	2303	0.91

\* Results deleted due to testing problems.

Averages		
Influent (ppm)	Effluent (ppm)	% Destruction
0.88	0.34	61.1

Ethylene Destruction

### Run 8

Time (min)	Probe 1 (ohms)	Temperature (°F)
0	14.84	44.69
7	14.52	45.57
12	14.65	45.23
18	14.48	45.69
22	14.38	45.97
27	14.49	45.66

Influent Temperatures

Time (min)	Probe 3 (ohms)	Temperature (°F)
0	14.39	45.20
7	13.78	46.88
12	13.61	47.38
18	13.20	48.50
22	13.04	48.93
27	13.01	49.02

Effluent Temperatures

Time (min)	Probe 2 / dry (ohms)	Temperature (°F)	Probe 2 / wet (ohms)	Temperature (°F)	Relative Humidity (%)
0	14.70	45.0	14.81	44.7	>90
25	14.45	45.7	14.74	44.9	>90

Influent Humidity

Time (min)	Probe 4 / dry (ohms)	Temperature (°F)	Probe 4 / wet (ohms)	Temperature (°F)	Relative Humidity (%)
0	14.48	45.3	14.78	44.5	>90
25	13.17	48.8	13.43	48.1	>90

Effluent Humidity

Inf / Eff	Needle	Time (min)	Ethylene (peak area)	Ethylene (ppm)
Influent	1	0	2071	0.82
Effluent	2	5	632	0.25
Effluent	3	10	390	0.15
Effluent	4	15	441	0.18
Influent	5	15	1625	0.64*
Effluent	6	20	354	0.14
Influent	7	25	1471	0.58*
Influent	8	30	1576	0.63*

\* Results deleted due to testing problems.

Averages		
Influent (ppm)	Effluent (ppm)	% Destruction
0.82	0.18	78.1

Ethylene Destruction

### Run 9

Time (min)	Probe 1 (ohms)	Temperature (°F)
0	14.91	44.49
7	14.88	44.57
12	14.73	45.00
18	14.84	44.69
22	14.73	45.00
27	14.59	45.37

Influent Temperatures

Time (min)	Probe 3 (ohms)	Temperature (°F)
0	13.64	47.29
7	13.38	48.00
12	13.20	48.50
18	13.02	49.00
22	12.95	49.20
27	13.02	49.00

Effluent Temperatures

Time (min)	Probe 2 / dry (ohms)	Temperature (°F)	Probe 2 / wet (ohms)	Temperature (°F)	Relative Humidity (%)
0	14.42	45.8	14.77	44.8	>90
25	14.66	45.1	14.70	45.0	>90

Influent Humidity

Time (min)	Probe 4 / dry (ohms)	Temperature (°F)	Probe 4 / wet (ohms)	Temperature (°F)	Relative Humidity (%)
0	13.95	46.7	14.26	45.9	>90
25	13.28	48.5	13.50	47.9	>90

Effluent Humidity

Inf / Eff	Needle	Time (min)	Ethylene (peak area)	Ethylene (ppm)
Influent	1	0	1960	0.78
Effluent	2	5	729	0.29
Effluent	3	10	802	0.32
Effluent	4	15	562	0.22
Influent	5	15	1625	0.64*
Effluent	6	20	658	0.26
Influent	7	25	2005	0.80

\* Results deleted due to testing problems.

Averages		
Influent (ppm)	Effluent (ppm)	% Destruction
0.79	0.27	65.3

Ethylene Destruction

### Run 10

Time (min)	Probe 1 (ohms)	Temperature (°F)
0	14.06	46.86
7	14.19	46.52
12	14.17	46.57
18	14.23	46.40
22	14.33	46.12
27	14.31	46.17

Influent Temperatures

Time (min)	Probe 3 (ohms)	Temperature (°F)
0	13.78	46.90
7	13.76	46.95
12	13.51	47.64
18	13.64	47.30
22	13.62	47.35
27	13.68	47.18

Effluent Temperatures

Time (min)	Probe 2 / dry (ohms)	Temperature (°F)	Probe 2 / wet (ohms)	Temperature (°F)	Relative Humidity (%)
0	14.38	45.9	14.74	44.9	>90
25	14.45	45.7	14.63	45.2	>90

Influent Humidity

Time (min)	Probe 4 / dry (ohms)	Temperature (°F)	Probe 4 / wet (ohms)	Temperature (°F)	Relative Humidity (%)
0	14.67	44.8	14.86	44.3	>90
25	13.88	46.9	14.22	46.0	>90

Effluent Humidity

Inf / Eff	Needle	Time (min)	Ethylene (peak area)	Ethylene (ppm)
Inf	6	0	204	0.08*
Eff	7	10	1643	0.65
Eff	8	20	1443	0.57
Inf	9	30	2511	1.00
Eff	10	30	1396	0.55

\* Results deleted due to testing problems.

Averages		
Influent (ppm)	Effluent (ppm)	% Destruction
1.00	0.59	40.5

Ethylene Destruction



### Run 11

Time (min)	Probe 1 (ohms)	Temperature (°F)
0	14.61	45.32
7	14.40	45.92
12	14.25	46.34
18	14.08	46.80
22	14.20	46.49
27	14.01	47.00

Influent Temperatures

Time (min)	Probe 3 (ohms)	Temperature (°F)
0	13.34	48.10
7	13.46	47.79
12	13.88	46.62
18	13.66	47.22
22	13.27	48.30
27	13.51	47.64

Effluent Temperatures

Time (min)	Probe 2 / dry (ohms)	Temperature (°F)	Probe 2 / wet (ohms)	Temperature (°F)	Relative Humidity (%)
0	14.63	45.2	14.81	44.7	>90
25	14.38	45.9	14.74	44.9	>90

Influent Humidity

Time (min)	Probe 4 / dry (ohms)	Temperature (°F)	Probe 4 / wet (ohms)	Temperature (°F)	Relative Humidity (%)
0	13.54	47.8	13.73	47.3	>90
25	13.62	47.6	13.65	47.5	>90

Effluent Humidity

Inf / Eff	Needle	Time (min)	Ethylene (peak area)	Ethylene (ppm)
Inf	1	0	2444	0.97
Eff	2	10	1437	0.57
Eff	3	20	1325	0.53
Eff	4	30	1267	0.50
Inf	5	30	2593	1.03

Averages		
Influent (ppm)	Effluent (ppm)	% Destruction
1.00	0.53	46.7

Ethylene Destruction

Ethylene  
(ppm)  
4.2  
2.0  
0.0

**Appendix F:**

**Closed Loop**

**Test Data**

Needle	Time (min)	Ethylene (peak area)	Ethylene (ppm)
1	0	1668	0.97
2	22	861	0.50
3	44	1008	0.59
4	66	900	0.52
5	110	1065	0.62
6	132	901	0.52
7	154	894	0.52
8	176	882	0.51

Closed Loop Test #1 Data

Needle	Time (min)	Ethylene (peak area)	Ethylene (ppm)
1	0	2277	
2	0	2300	
3	0	2308	
4	0	2138	0.90*
5	24	1776	0.70
6	48	1316	0.52
7	72	1081	0.43
8	96	1192	0.47

\* Indicates an average of several points.

Closed Loop Test #2 Data

Needle	Time (min)	Ethylene (peak area)	Ethylene (ppm)
1	0	1139	
2	0	1383	
3	0	1230	
4	0	1158	0.49*
5	24	1063	0.42
6	48	901	0.36
7	72	778	0.31
8	96	972	0.39

\* Indicates an average of several points.

Closed Loop Test #4 Data

Needle	Time (min)	Ethylene (peak area)	Ethylene (ppm)
1	0	1978	
2	0	2024	
3	0	2100	0.81*
4	120	1258	0.50
5	132	1342	0.53
6	144	1187	0.47

\* Indicates an average of several points.

Closed Loop Test #5 Data

Needle	Time (min)	Ethylene (peak area)	Ethylene (ppm)
1	0	2036	
2	0	2140	0.83*
4	120	1632	0.65
5	132	1662	0.66
6	144	1643	0.65
7	156	1622	0.64
9	180	1650	0.65
10	192	1507	0.60

\* Indicates an average of several points.

Closed Loop Test #6 Data

2

## VITA

**Thomas K. Graham**

Candidate for the Degree of Master of Science

**Thesis:** DESTRUCTION OF ETHYLENE IN A LIQUID ELECTRODE PLASMA REACTOR

**Major Field:** Environmental Engineering

**Personal Data:** Born in Miami, Oklahoma, May 8, 1973; Raised in Hominy, Oklahoma; the son of Marion and Linda Graham

**Education:** Graduate of Hominy High School - May 1991

Bachelor of Science degree in Civil and Environmental Engineering, from Oklahoma State University; Stillwater, Oklahoma - December 1995

Completed the requirements for the Master of Science degree with a major in Environmental Engineering at Oklahoma State University - May 1997

**Experience:** Worked for Oklahoma State University as a *Teaching Assistant* and *Research Assistant* from 1991 to 1997. Served as a summer *Engineering Intern* at the USDA Hydraulics Laboratory located in Stillwater, Oklahoma. Raised on a family ranch near Hominy, Oklahoma.

### Professional

**Memberships:** National Society of Professional Engineers  
American Society of Civil Engineers  
Phi Mu Alpha Sinfonia  
Phi Kappa Phi

**Registration:** Engineering Intern - Oklahoma Registration No. 10123

**Honors/Awards:** Outstanding Graduate for the College of Engineering - 1996  
ASCE, Oklahoma Section, Outstanding Graduate - 1996  
Top Five Senior Male at OSU - 1996  
Who's Who Among American Colleges and Universities